Genomic data suggest environmental drivers of fish population structure in the deep sea; a case study for the orange roughy (*Hoplostethus atlanticus*)

Anders Gonçalves da Silva[1,†], William Barendse[2], James Kijas[2], Phillip R. England[1], A. Rus Hoelzel[3,*]

[1] CSIRO Hobart, Castray Esplanade, Battery Point TAS 7004, Australia

[2] CSIRO Agriculture, 306 Carmody Rd, St Lucia QLD 4067, Australia

[3] Department of Biosciences, University of Durham, South Road, Durham DH1 3LE, UK

[†] Current address: Microbiological Diagnostic Unit Public Health Lab, Peter Doherty Institute (Bldg 248) The University of Melbourne Parkville, VIC 3010, Australia

[*] Corresponding author: a.r.hoelzel@durham.ac.uk

Keywords: Conservation genetics, deep sea, natural selection, isolation by distance, fisheries

Abstract

1. The accurate identification of conservation units is central to effective management strategies. However, marine environment populations often have large census sizes and few obvious boundaries to gene flow. Poorly understood species in the deep sea are especially at risk of being erroneously managed as a single interbreeding stock (panmictic). However, mistaking cryptic structure for panmixia can have important consequences leading to ineffective management and population decline. Furthermore, characteristics of populations essential for their survival may reflect local adaptation, not evident from surveys using neutral genetic markers.
2. We use genomic methodologies to test hypotheses about potential drivers of cryptic population structure among marine fish populations in the deep sea. In particular, we consider the possibility of isolation by distance (IBD) along habitat corridors for a species dependent on a specific depth range, and test for differentiation at functional loci across potential ecological habitat boundaries.
3. For a species previously understood to be panmictic in the North Atlantic we reveal neutral genetic differentiation among regional populations isolated by distance along deep-water channels. We also reveal a distinct pattern of cryptic genetic structure for putative functional loci, despite apparently high levels of gene flow.
4. *Synthesis and applications*. This example reflects the life history and ecology of a broad range of deep-sea species currently exploited in intensive fisheries or as by-catch. In many cases where these populations are managed as a single stock, more effective management could be achieved using the methods we describe to identify relevant eco-evolutionary processes, facilitated by genomic methods, permitting the recognition of cryptic stock structure. This approach also allows managers to more directly promote the essential but elusive conservation of adaptive potential.

1 | INTRODUCTION

Understanding the process of evolution in the context of ecological and biogeographic factors is fundamental for the effective, predictive identification of appropriate units of conservation and management. In support of these objectives, we are now able to generate vast quantities of genomic data. The initial reactions to this flood of data were that it would be transformative, in particular for the management of commercially-exploited species, or those under considerable threat of extinction (e.g. Allendorf *et al.* 2010). More recently, some skepticism has been expressed, questioning the necessity of genomic data for basic applications in conservation biology, and noting that our ability to interpret aspects of those data (especially the role of natural selection) remains in an early stage of development (Shafer *et al.* 2015). However, exceptions were soon noted (see Garner *et al.* 2016; Shafer *et al.* 2016).

One clear advantage for genomic methods compared to the earlier methods using allozymes, short sequences of DNA or microsatellite DNA genotypes (see Waples 1998; Hauser & Carvalho 2008) is the increase in power. This power can potentially reveal very low levels of gene flow, which raises questions about the conservation relevance. In cases where life history, demography or phenotype suggest a need for separate stock management, but even thousands of neutral loci derived from genome sampling methods show little or no structure (e.g., Gonçalves da Silva *et al.* 2015a) there may need to be a change in paradigm for how genetic data are used in conservation and management (Hauser & Carvalho 2008; Ovenden *et al.* 2015). One suggestion has been to focus on the demographic independence of stocks (Palsbøll *et al.* 2007), and simulations show that correlated demography can require quite high migration rates (in the range of 0.1-0.3), high enough to result in very small values of structure based on F_{ST} (White *et al.* 2011). In this context, the high resolution is important

because it permits the detection of independence to a level of resolution consistent with these high levels of gene flow.

Another approach focuses on identifying what we previously called *evolutionarily compatible* stocks (Gonçalves da Silva *et al.* 2015a). These are stocks for which individuals are exchangeable, by which we mean there are reasonable expectations that a translocated individual would exhibit similar growth rates to local individuals, as is often assumed (Hauser & Carvalho 2008). This might occur because the environment is relatively uniform across stocks, or when selective pressure reflecting environmental differences is not sufficient to overcome the homogenizing effects of high levels of gene flow. However, cryptic environmental structures or local adaptation may generate evolutionarily incompatible stocks that will require identification and management as separate conservation units.

We chose orange roughy for this study because of earlier data indicating panmixia (White et al. 2009), its habitat dependences and its history of exploitation (characteristics shared by many species of conservation concern). Genetic data currently available suggested effective panmixia across ocean basins (Oke *et al.* 2002; White *et al.* 2009; Gonçalves da Silva *et al.* 2015a). Attempts to delimit stocks off Australia using parasites, morphology, otolith biochemistry, and numerous genetic markers sometimes suggested structure, but did not always produce consistent and reproducible boundaries (see review in Gonçalves da Silva *et al.* 2015a). This species dwells in the deep sea at depths that range from ~500 to 1,800 m, breeds on sea mounts, and can live for over 100 years (see review in White et al. 2009). It has been heavily exploited with stocks reduced by an estimated 80% in some regions (e.g. Clark et al. 2000).

Orange roughy populations span diverse habitats and environmental conditions (for example across the thermal boundary at the sub-polar front). As for other species in the pelagic and deep sea environments, rather than being continuously distributed across the

North Atlantic, they could instead be a collection of highly interconnected populations, distinguished by locally adapted loci. An example of such a situation can be found in the cod (*Gadus morhua*) populations of the Baltic and North seas (Nielsen *et al.* 2009). These populations are indistinguishable at neutral loci, but show distinct signatures of local adaptation that are presumed to be related to the gradients of temperature and salinity observed between the two seas. Genome sequencing has also revealed a clear example of local adaptation in Atlantic herring (*Clupea harengus*) which differ in their reproductive timing and adaptation to salinity (Martinez-Barrio et al., 2016), and American lobster (*Homarus americanus*) showing variation correlated to sea surface temperature (Benestan et al. 2016).

Here we apply population genomic analyses using SNP (single nucleotide polymorphic) loci and uncover population structure relevant to the management of this and potentially for other widely dispersed species in the deep sea. We focus on ecological differences among putative populations, and the biogeographic patterns that emerge when we track genetic differentiation along habitat contours. First, we test the hypothesis that habitat use in a complex environment (which may be based on factors such as preference or dependence) has led to cryptic patterns of dispersion and isolation by distance. Second, we test the hypothesis that environmental discontinuities are associated with differential patterns of local adaptation, despite apparently high levels of gene flow. The latter analysis addresses questions about the feasibility of identifying diversity relevant to adaptive potential (see Shafer *et al.* 2015), a key, long-standing objective of conservation genetics, rarely fulfilled. Together these analyses provide consequential inference in support of the more effective management of this and similar species in the deep sea.

2 | MATERIAL AND METHODS

2.1 | Sample collection and DNA extraction

Tissue and blood samples were collected as described by White *et al.* (2009) and Gonçalves da Silva *et al*. (2015b). Sampled locations included two in the South Atlantic (off the west coast of Namibia and South Africa) , and six in the North Atlantic (two on the mid-Atlantic Ridge, and four along the west coast of UK and Europe; Fig 1; Table 1). Total DNA was isolated using a phenol:chloroform-based protocol described by Hoelzel & Green (1998) for samples described in White *et al.* (2009). Additional samples obtained later were extracted using a modified QIAGEN DNeasy protocol described in Gonçalves da Silva *et al*. (2015a). All samples were collected post-mortem from fish taken in fisheries or during independent fisheries research activities. No permits were required.

2.2 | DNA analysis and quality control

Genetic variation was assessed using 4723 variable SNPs described by Gonçalves da Silva *et al.* (2015b) using an Illumina HD Infinium® custom array (Illumina, Inc., USA) following the manufacturer's recommended protocol. We used 4 µl of DNA with a concentration between 20 and 400 ng/µl for each genotyping assay. Arrays were scanned on a HiScanSQ (Illumina, Inc., USA).

Sample and locus quality were first assessed using Illumina software (Illumina GenomeStudio, v.2011.1; Illumina, Inc., USA). Subsequently, we removed monomorphic loci, and determined a set of loci considered to be in Linkage Equilibrium (LE) and Hardy-Weinberg Equilibrium (HWE) across the sampled locations (Populations). Details can be found in Gonçalves da Silva *et al.* (2015b) and in Supporting Information (Figs S1-S5, Tables S1-S2).

2.3 | Identifying outlier loci

We employed four methods to identify outlier loci: *PCAdapt* (Duforet-Frebourg *et al.* 2014), *BayesEnv2* (Günther & Coop 2013), *Lositan* (Antao *et al.* 2008) and *BayeScan* (Foll & Gaggiotti 2008). The methods employ different approaches, and make distinct assumptions about the processes that generate the data (see supplementary methods). Results were compared across methods in order to minimize issues related to our poor knowledge of the species' demographic history and spatial distribution of genetic variation (Lotterhos & Whitlock 2014).

2.4 | Identifying outlier loci potential functional context

We used the relatively small and strict sample of outliers detected in BayeScan to further explore possible functions associated with local selection. We began by compiling a database of teleost protein sequences from NCBI *RefSeq* database. We then used *blastx* to search this database using the contigs where the single nucleotide polymorphisms (SNPs) were identified as a query. We performed three searches, each with a different amino acid substitution matrix: BLOSUM45, 62 and 80. This allowed for both divergent and closely related proteins to be mapped to our contigs. The output of the *blast* search was converted to a *GFF* file, which included the SNP location, and visualized in Geneious.

2.5 | Describing population structure

We report results for two sets of loci used to describe the population structure of our orange roughy samples: (1) loci that were found to be outliers in at least one of the four methods; and (2) loci found to be neutral in all four methods. We calculated global and pairwise Weir and Cockerham's (1984) F_{ST} values for each dataset using GENETIX version 4.05 (Belkhir *et al.* 1996). Significance was assessed by permuting genotypes 10,000 times. In addition, we produced a low-dimensional graphical representations of the population

structure using factorial correspondence analysis (FCA) in GENETIX, and discriminant analysis of principal components (DAPC; Jombart *et al.* 2010) using *adegenet* version 2.03 (Jombart & Ahmed 2011) in *R* (R Core Team 2016). For the FCA we examined the top three factors. For DAPC, we used the *optim.a.score* function to identify an optimal number of principal components to keep in order to avoid overfitting (Jombart *et al.* 2010). We visually inspected all 2D combinations of the DAPCs. Sampling locations were used as the prior groupings for DAPC.

Both FCA and DAPC analyses of neutral loci suggested the possibility of isolation-by-distance within North Atlantic (NA) populations. We generated pairwise geographic distances for three possible scenarios: (1) minimum pairwise distance between sampling locations taking into account only the Earth's curvature; (2) minimum pairwise distance between sampling locations such that paths had to be at least 10m in depth, thus avoiding land masses; and (3) minimum pairwise distance between sampling locations such that paths were constrained to follow bathymetric contours between 500 and 2500m in depth, thus limiting to paths thought to be within biologically reasonable depths for the species. We then calculated pairwise genetic distances between locations using the centroid for each sampled location along the second DAPC (which differentiated NA sampling locations). Pearson's correlation coefficient (r) was calculated between the genetic distance matrix and each geographic distance matrix, and its significance estimated by 10,000 permutations of the genetic distance matrix (Legendre & Fortin 2010). Minimum geographic distances were obtained using *marmap* package (Pante & Simon Bouhet 2013) in *R* (R Core Team 2016).

2.6 | Geogenetic distances

Using neutral loci, we ran SpaceMix (version 0.12) as described in Bradburg et al. (2016). SpaceMix produces geogenetic coordinates, which are geographic coordinates

192 distorted by, or corrected for, gene flow (i.e., the greater the gene flow, the closer locations
193 will appear in the geogenetic map). To facilitate pattern detection we used the "target" model
194 (mapping from the source of admixture to its target on the inferred map; see
195 https://github.com/gbradburd/SpaceMix/blob/master/vignettes/spacemix_vignette.Rmd) to
196 estimate the geogenetic coordinates of our North Atlantic samples. We ran 50 fast replicates
197 to train the MCMC, each with 1 million steps, and then a single long chain with 10 million
198 steps. We performed the suggested posterior checks, assessing concordance and MCMC
199 convergence.
200 To examine different geogenetic distance hypotheses, we calculated the pairwise
201 distance from Bay of Biscay to each of the other five sampling locations in the North Atlantic
202 for each posterior sample from the MCMC. Under a hypothesis of isolation-by-distance along
203 the continental shelf towards Iceland, and then across to the mid-Atlantic ridge, we expect the
204 geogenetic distances to increase from Bay of Biscay in the following order: Porcupine Bank,
205 Scotland, Hebrides, Faraday Seamount, and then Sedlo Bank. In other words, the geogenetic
206 distance between Bay of Biscay and Porcupine Bank would be the smallest, then the distance
207 between Bay of Biscay and Scotland, and so forth. Under a hypothesis that the Gulf Stream
208 has an appreciable effect in determining gene flow in orange roughy, however, we might
209 expect that Sedlo Bank and Faraday Seamount would be closer to continental shelf locations
210 than they would be to each other.
211 There are 120 possible permutations of the order in which the pairwise geogenetic
212 distance can increase from a focal population. We chose Bay of Biscay as our focal
213 population because it is at one extreme of the distribution of sampling locations. For each of
214 the 120 permutations, we counted the number of times that order appeared in the posterior
215 sample. When normalized by the total number of posterior samples, this provides us with a
216 measure of the relative plausibility of any particular order given our data.

3 | RESULTS

3.1 | Detecting outliers

Based on our assessment of genotype quality, linkage and Hardy-Weinberg Equilibrium, and signatures of ascertainment bias we identified 4,179 loci that were variable in our dataset, and met all quality criteria (see Supplementary methods).

Across all four employed outlier detection methods we identified 420 outlier loci when considering the most inclusive criteria for defining outliers (Table 2). Detailed illustrations for each method are provided in the supplementary file (Figs S6-S13). Of these 420 outliers 232 were identified by at least two methods; 131 by at least three methods; and 52 were identified by all four methods (Fig S14). Bayescan had the fewest number of identified outlier loci (Fig S8), even when the prior odds of a neutral model over a selection model was only 10:1. The other three methods identified over 200 loci each (209, 281, and 281, respectively for BayEnv2, Lositan, and PCAdapt). Congruence was up to 91%, but generally lower (Fig S14). See Supplementary Information for detailed results of comparative analyses.

The posterior distribution of F_{ST} (the probability that two alleles taken at random from a population have an ancestor in that population), suggests structure between South and North Atlantic, as well as within the North Atlantic (Fig 2). The two populations from the South Atlantic are clear outliers (mean F_{ST} ~ 0.025 for Namibia and South Africa, compared to an overall mean across all populations of 0.007). Within the North Atlantic, we see an increase in F_{ST} along the coastal margin populations from Hebrides in the North to Bay of Biscay in the South (the posterior mean increases from 0.0010 to 0.0016). Finally, the two mid-Atlantic ridge populations have mean F_{ST} of 0.0025 and 0.0056 for Sedlo Bank and Faraday Seamount, respectively.

3.2 | Outlier loci function

Among the eight strongest outliers identified from the BayeScan analysis, three of those SNPs were on contigs that contained regions matching fish protein sequences. None of the SNPs were found within coding regions. Using the BLOSUM80 matrix against the fish protein database, one SNP was found in a putative intronic region (SNP: 1405747-4_245) of a gene (ARR2) described as being part of a sensory transduction biological pathway in rainbow trout (*Oncorhynchus mykiss*; GO:0050896; UniProt:P51467). Another (SNP: 808350-0_624) was found 1750bp upstream of a protein (EXT1C) characterized as part of the biosynthesis pathway of heparan sulfate in zebrafish (*Danio rerio;* GO:0015012; UniProt: Q5IGR6). Finally, one SNP (SNP: ID: 1108376-13_704) was found 14,192 bp downstream of a protein (PSPC1) involved in regulating biological rythyms (GO:0042752; UniProt: Q1JPY8) in *Danio rerio*.

3.3 | Population structure

Measures of population diversity and comparisons against Hardy Weinberg expectations are given in Table 1. As suggested by Narum (2006), we applied the Benjamini & Yekutieli (2001) correction for multiple testing to all tests of the null hypothesis that pairwise $F_{ST} = 0$, resulting in a corrected *p*-value of 0.0127 ($0.05/(\sum_{i=1}^{28} \frac{i}{28})$). Pairwise F_{ST} using loci found to be neutral across all four outlier detection methods (Table 3) was significantly larger than zero for all pairwise comparisons between North and South Atlantic (mean $F_{ST} = 0.0103$, sd = 0.00061). The within South Atlantic (SA) pairwise F_{ST} was not different from zero ($F_{ST} = 0.00004$). The mean pairwise F_{ST} across NA sampling locations was 0.00063 (sd 0.00067), and three pairwise comparisons were significant (Table 3). Pairwise F_{ST} using loci found to be outliers in at least one of the outlier detection methods

(Table 3) were also significantly larger than zero for all comparisons between NA and SA (mean F_{ST} = 0.077, and sd = 0.00064). F_{ST} for outlier loci between the SA sampling sites was not different from zero, while in the NA most comparisons were significant (Table 3).

When running DAPC we found that keeping 19 PCs was optimal in order to avoid overfitting. Both FCA and DAPC resulted in similar representations of the population structure for both neutral and outlier loci (Fig 3). Across all four panels, the differentiation between NA and SA is captured along the first dimension. The second dimensions of the neutral loci panels suggest differentiation among the NA sampling locations. In the outlier panels, the second dimension singles out Faraday Seamount as divergent from all other NA sampling locations (Fig 3). This pattern was also detected when only the outlier loci from a single method were included (see Fig S15). Tests of smaller subsamples from the 420 combined outlier loci show that 50 loci are too few for strong inference (see Fig S16), and so we could not gain useful interpretation from analyses of the 52 outlier loci shared among all four methods (see Fig S14).

3.4 | Isolation-by-distance

Our tests for isolation-by-distance (IBD) found a strong relationship between pairwise distances along paths constrained to bathymetric contours between 500m and 2500m in depth and pairwise genetic distances as measured by the second DAPC (R^2 = 0.43; *p*-value = 0.0051; Fig 4). The other comparisons were not significant, and no significant relationships were identified with outlier loci (data not shown).

Of the 120 possible permutations of order analyzed for geogenetic distances, only 30 were observed in our posterior sample of 999. The 95% credible interval included 10 possible orders, with four comprising over 80% of the posterior mass. The 95% credible interval supports a hypothesis of isolation-by-distance along the continental shelf, as seen above using

292 the Mantel test (Fig 4). There is some uncertainty about the ultimate order of the sampling
293 locations, in particular between Hebrides and Scotland, and between Faraday Seamount and
294 Sedlo Bank. Nevertheless, either Faraday Seamount or Sedlo Bank were always the furthest
295 on the geogenetic scale from Bay of Biscay in the 95% credible set.
296
297 **4 | DISCUSSION**
298 A key objective of conservation is to preserve the potential for species to survive and
299 retain their natural diversity into the future, facilitating adaptation to a changing world. The
300 spectrum of essential conservation work is broad, including crisis issues associated with
301 endangered species, but also including established populations where the risk is less known or
302 cryptic. Exploited marine fish species commonly show low levels of population structure and
303 have large census numbers (with many thousands of tons of fish taken for some species
304 annually), but they also often have small Ne/Nc ratios (Hare *et al.* 2011). The effective
305 population size (Ne) is the size of an idealized population that would show the same rate of
306 loss of diversity as the observed population, while Nc is the census number. Therefore, Ne is
307 the evolutionarily relevant population size, and associated with the rate at which diversity is
308 lost. Furthermore, even very low levels of differentiation among populations may provide
309 information important to effective management (White *et al.* 2010), especially when
310 populations are demographically independent (Waples *et al.* 2008) or differentiated by local
311 adaptation. In this study we reveal evolutionarily incompatible populations for a species
312 previously understood to be panmictic in the North Atlantic (White *et al.* 2009) by deploying
313 methods that provide high resolution and permit the assessment of adaptive diversity. We
314 furthermore propose an association with two environmental characteristics potentially
315 generating population structure in this system: a thermal transition at the sub-polar front,
316 south of which we find evidence for local adaptation (in the Faraday Seamount population),

317 and a pattern of depth contours across the eastern North Atlantic associated with genetic
318 isolation by distance (IBD).

319 Our comparisons between Namibia and South Africa showed little structure, with only
320 FCA able to differentiate among the two sampling locations. However, in the North Atlantic
321 neutral markers showed genetic differentiation as a pattern of IBD increasing along a path that
322 follows 500m to 2500m depth contours (which encompasses the ~900-1800m core habitat
323 range of the species; Fig 4). Although we did not quantify ocean current trajectories for this
324 model, the general pattern of current flow at depth is broadly coincident with but not identical
325 to the path we identified (Reid 1994; Marzocchi *et al.* 2015).

326 Modelling by Spies *et al.* (2015) demonstrated that IBD should not be ignored when
327 there is spatial variation in hunting pressure, and the spatial scale of management is larger
328 than the mean lifetime dispersal distance (i.e., the scale at which genetic drift becomes
329 stronger than gene flow; Hutchison & Templeton 1999). In that case they recommended that
330 the management area be subdivided to the scale of each deme. Fishing areas in the North
331 Atlantic are designated into FAO (food and agriculture organization of the United Nations)
332 fishing zones (FAO 2017), which are managed by the North East Atlantic Fisheries
333 Commission (NEAFC). NEAFC groups deep-sea fisheries together and defines a
334 management area that encompasses the broader geographic region investigated in our study
335 (see https://www.neafc.org/managing_fisheries/measures/current). Species-specific
336 management can be developed "pending ICES [International Council for the Exploration of
337 the Sea] advice facilitating stock specific measures". However, if there is an IBD structure
338 within a designated stock, this would risk the economic viability of the fishery and long-term
339 conservation under the modelling of Spies *et al*. (2015).

340 For the orange roughy the most recent ICES report (ICES WGDEEP Report 2018,
341 document 09; see https://www.ices.dk/sites/pub/) states that "There is no information to

342 determine the existence of separate populations of orange roughy in the North Atlantic."
343 However, they designate subareas 6 and 7 (where there have been documented declines for
344 this species since the early 1990s) together with the 'rest of the region' as the current
345 assessment units. Our data are consistent with the designation of subareas 6 (our North
346 Rockall and Hebrides samples) and 7 (our Porcupine Bank sample) given the separate genetic
347 clusters identified from our analyses (see Fig. 3). However the 'rest of the region' together
348 with subareas 6&7 show an IBD pattern of diversity (see Fig. 4). The putative population at
349 Faraday Seamount, where we found evidence for local adaptation, is outside the NEAFC
350 management region, but within the mid-Atlantic ridge marine protected area (see O'Leary et
351 al. 2012). In general, management strategies often define spatial stock boundaries as the units
352 of conservation. We show that high resolution genomic methods can identify more complex,
353 previously unrecognized, patterns of demographic and genetic structure, relevant to effective
354 conservation.

355 The most likely models for IBD patterns will depend on whether dispersal is primarily
356 at the larval or adult stage. For example, in a species with an extended larval phase and
357 buoyant eggs, dispersal may follow major current patterns (e.g. as for Greenland halibut;
358 *Reinhardtius hippoglossoides* in the North Atlantic, Knutsen et al. 2007). Adult dispersal was
359 proposed for orange roughy by White *et al.* (2009), and would fit with inferred spawning
360 migrations for orange roughy in New Zealand (Clark *et al.* 1998) and Australia (Upston &
361 Wayte 2012). From our data the supported IBD model was along a path that reflected the
362 adult habitat depth range, and so was consistent with adult dispersal. An association between
363 dispersal pattern and bathymetry was also reported for cusk (*Brosme brosme*) across a similar
364 geographic range (Knutsen et al. 2007). However, the current patterns follow a similar route
365 (Reid 1994; Marzocchi *et al.* 2015; see Fig 4) and orange roughy eggs last up to 30 days, so
366 both adult and larval (Dunn *et al.* 2009) dispersal could be consistent with our data.

Some preliminary data suggest that juvenile orange roughy may have a distribution that is more mesopelagic than the adults in the North Atlantic, based on stable isotope data from 11 samples (Shephard et al. 2007). Our data reflecting local adaptation in adults may therefore represent populations of individuals that had a broader or distinct distribution at earlier life history stages. An interesting parallel example may be the depth distribution of the roundnose grenadier (*Coryphaenoides rupestris*) in the eastern North Atlantic, where sympatric juveniles of distinct genotypes at specific functional loci (with fixed non-synonymous variants) segregate to different depths as adults depending on their genotype (Gaither et al. 2018). Carlsson et al. (2011) also suggest subtle genetic differentiation (F_{ST} = 0.004-0.01) from the Porcupine Bank area comparing samples from 'flat' and 'mound' habitats during spawning periods based on 8 microsatellite DNA loci. However, there was just one flat site compared to 6 mound sites, and some mound sites were also differentiated from each other with F_{ST} values of a similar magnitude. In our dataset the differentiated samples comparing the Hebrides and the Bay of Biscay were both sampled from mound sites during spawning periods (see White et al. 2009).

Central to the concept of evolutionarily compatible populations is the idea that populations that share the same adaptations would be interchangeable, and that overexploitation in one area could be compensated for by immigration from another area. However, as illustrated by our results for the North Atlantic orange roughy populations, the pattern of apparent connectivity can differ for neutral compared to putative functional loci (see Fig 3). The population at Faraday Seamounts stands out in ordination analyses based on putative functional loci, and so a precautionary approach should assume that interchange with this population is not evolutionarily compatible due to local adaptation. We identify several outlier SNPs that showed proximity to coding loci with potentially relevant GO terms, however further data will be needed to identify specific relevant functional changes. A

392 significant environmental boundary separates this population, the sub-polar front reflecting a
393 thermal transition and associated environmental differences (potentially relevant for other
394 species of conservation concern as well). Although we cannot yet demonstrate a causative
395 relationship between this thermal transition and adaptive genetic differentiation for this
396 species, the association suggests a need for further assessment in support of effective
397 conservation, and similar associations with thermal habitats have been reported for other
398 marine systems (e.g. Benestan et al. 2016).

399 Distinct inference from neutral and adaptive markers have suggested important
400 boundaries for conservation in a few other studies (e.g. Nielsen et al. 2009, Benestan et al.
401 2016), but these data are still relatively rare. At the same time, we expect that further high
402 resolution research will reveal many more examples, and propose that the identification of a
403 distinct pattern of connectivity for putative functional diversity compared to that seen at
404 neutral loci should be sufficient to indicate cryptic genetic diversity in support of genetic
405 stock management designation and further assessment. This would involve the consideration
406 of stock designations for the preservation of local adaptive characteristics independent of the
407 level of movement, since selection can maintain the difference despite ongoing gene flow
408 through dispersal (e.g. Gaither et al. 2018).

409 Conservation genetics has focused on demographic inference and neutral models
410 essentially since its inception. However, a major objective has always been the conservation
411 of adaptive potential, more recently referred to as 'evolutionary conservation' (see Eizaguirre
412 & Baltazar-Soares 2014). Inference about population structure and demography based on
413 neutral loci has provided an important contribution to more effective conservation (e.g.
414 Hauser & Carvalho 2008), potentially extended by high-resolution testing of eco-evolutionary
415 hypotheses, as illustrated by our results reported here on cryptic IBD. However, relatively
416 few studies have addressed the question of adaptive potential, an increasingly critical issue in

the face of anthropogenic environmental change. A number of studies have considered phenotypic variation and additive variance, recognizing the importance of large Ne (e.g. Hoffman et al. 2017), but the identification of loci critical to the conservation of local adaptation has lagged behind, largely due to limitations in technology (see Shafer et al. 2015). Here we illustrate the potential for relatively low-cost genomics to provide useful inference about local adaptation, even without knowing specific gene function. The synthesis of eco-evolutionary theory, high resolution population genomics, and contrasting population structure at neutral and functional loci will reveal cryptic patterns of structure that need to be conserved if evolutionary potential is to be maintained in managed populations.

ACKNOWLEDGEMENTS

We wish to thank Francis Neat and Marine Scotland for providing us with orange roughy samples from Scottish coast, Marine Girard, Pascal Lorance, and Odd Aksel Bergstad and the MARECO team for help in acquiring the rest of the North Atlantic samples. We also thank Rob Leslie (DAFF, South Africa), David Japp and Melanie Smith (CapFish, South Africa) for orange roughy samples from the South African western coast and Arved Staby for samples from Namibia. We thank Joanne Stamford for help with DNA extractions. AGS would like to acknowledge a CSIRO Professional Development grant that allowed for collaboration with ARH. We thank the Leverhulme Trust for their support (research fellowship awarded to ARH). We would like to acknowledge Sharon Appleyard, Russell McCullough, Blair Harrison, and Rowan Bunch for assistance in the lab.

AUTHORS' CONTRIBUTIONS

ARH, PRE and AGS designed the research and AGS & ARH wrote the paper with input from co-authors. AGS performed the research and most analyses, aided by WB, JK & ARH.

DATA ACCESSIBILITY

All SNP data has been made available at the University of Melbourne's Figshare service and can be downloaded from DOI: https://doi.org/10.26188/5d9bc8afa5b54. All sequencing read data are available at NCBI under the BioProject PRJNA263690:

https://www.ncbi.nlm.nih.gov/bioproject/PRJNA263690

REFERENCES

Allendorf FW, Allendorf FW, Hohenlohe PA, Luikart G. 2010. Genomics and the future of conservation genetics. Nature Reviews Genetics **11**:697–709.

Antao T, Antao T, Lopes A, Lopes RJ, Beja-Pereira A, Luikart G. 2008. LOSITAN: A workbench to detect molecular adaptation based on a F-st-outlier method. BMC Bioinformatics **9**:323.

Belkhir K, Borsa P, Chikhi L, Raufaste N, Bonhomme F. 1996. GENETIX 4.05, logiciel sous Windows TM pour la génétique des populations. Laboratoire génome, populations, interactions, CNRS UMR **5000**:1996–2004. 1996–2004, Université de Montpellier II.

Benestan L, Quinn BK, Maaroufi H, Laporte M, Clark FK, Greenwood SJ, Rochette R, Bernatchez L. 2016. Seascape genomics provides evidence for thermal adaptation and current-mediated population structure in American lobster (Homarus americanus). Molecular Ecology **25**:5073–5092. Wiley/Blackwell (10.1111).

Benjamini Y, Yekutieli D. 2001. The control of the false discovery rate in multiple testing under dependency. The Annals of Statistics **29**:1165–1188. Institute of Mathematical Statistics.

Bradburd GS, Ralph PL, Coop GM. 2016. A spatial framework for understanding population structure and admixture. PLoS genetics **12**:e1005703 EP —70. Public Library of Science.

Carlsson J, Shephard S, Coughlan J, Trueman CN, Rogan E, Cross TF. 2011. Fine-scale population structure in a deep-sea teleost (orange roughy, *Hoplostethus atlanticus*). Deep-sea Research I 58: 627-636.

Clark MR, Anderson OF, Chris Francis RIC, Tracey DM. 2000. The effects of commercial exploitation on orange roughy (Hoplostethus atlanticus) from the continental slope of the Chatham Rise, New Zealand, from 1979 to 1997. Fisheries Research **45**:217–238.

Clark MR, Francis RICC, Clark M. 1998. Inferring spawning migrations of orange roughy (*Hoplostethus atlanticus*) from spawning ogives. Marine and freshwater Research **49**:103–108. CSIRO.

Duforet-Frebourg N, Bazin E, Blum MGB. 2014. Genome scans for detecting footprints of local adaptation using a Bayesian factor model. Molecular Biology and Evolution **31**:msu182–2495. Oxford University Press.

Dunn MR, Rickard GJ, Sutton PJH, Doonan IJ. 2009. Nursery grounds of the orange roughy around New Zealand. ICES Journal of Marine Science **66**:871–885.

Eizaguirre C & Baltazar-Soares M. 2014. Evolutionary conservation - evaluating the adaptive potential of species. Evolutionary Applications. **7**: 963-967

FAO. 2017, January 30. FAO Major Fishing Areas. ATLANTIC, NORTHEAST (Major Fishing Area 27). CWP Data Collection. Rome. Available from http://www.fao.org/fishery/area/Area27/en.

Foll M, Gaggiotti O. 2008. A genome-scan method to identify selected loci appropriate for both dominant and codominant markers: a Bayesian perspective. Genetics **180**:977–993.

Garner BA et al. 2016. Genomics in Conservation: Case Studies and Bridging the Gap between Data and Application. Trends in Ecology & Evolution **31**:81–83. Elsevier.

Gaither MR, Gkafas GA, de Jong M, Sarigol F, Neat F, Regnier T, Moore D, Gröcke DR, Hall N, Liu X, Kenny J, Lucaci A, Hughes M, Haldenby S, Hoelzel AR. 2018. Genomics of habitat choice and adaptive evolution in the deep sea. Nature Ecology & Evolution **2**: 680–687

Gonçalves da Silva A, Appleyard SA, Upston J. 2015a. Establishing the evolutionary compatibility of potential sources of colonizers for overfished stocks: a population genomics approach. Molecular Ecology **24**:564–579. Available from http://onlinelibrary.wiley.com/doi/10.1111/mec.13046/full.

Gonçalves da Silva A et al. 2015b. SNP discovery in nonmodel organisms: strand bias and base-substitution errors reduce conversion rates. Molecular Ecology Resources **15**:723–736.

Günther T, Coop G. 2013. Robust identification of local adaptation from allele frequencies. Genetics **195**:205–220.

Hare MP, Nunney L, Schwartz MK, Ruzzante DE, Burford M, Waples RS, Ruegg K, Palstra F. 2011. Understanding and estimating effective population size for practical application in marine species management. Conservation biology : the journal of the Society for Conservation Biology **25**:438–449. Available from http://onlinelibrary.wiley.com.ezp.lib.unimelb.edu.au/doi/10.1111/j.1523-1739.2010.01637.x/full.

Hauser L, Carvalho GR. 2008. Paradigm shifts in marine fisheries genetics: ugly hypotheses slain by beautiful facts. Fish and Fisheries **9**:333–362.

Hoelzel AR, Green A. 1998. PCR protocols and population analysis by direct DNA sequencing and PCR-based DNA fingerprinting. Pages 201–235 in A. R. Hoelzel, editor. Molecular genetic analysis of populations: a practical approach. IRL Press at Oxford University Press, Oxford.

Hoffmann AA, Sgro CM, Kristensen TN 2017. Revisiting adaptive potential, population size, and conservation. Trends in Ecology and Evolution **32**:506-517.

Hutchison DW, Templeton AR. 1999. Correlation of pairwise genetic and geographic distance measures: inferring the relative influences of gene flow and drift on the distribution of genetic variability. Evolution **53**:1898–1914. Society for the Study of Evolution.

Jombart T, Ahmed I. 2011. adegenet 1.3-1: new tools for the analysis of genome-wide SNP data. Bioinformatics **27**:3070–3071. Oxford University Press.

Jombart T, Devillard S, Balloux F. 2010. Discriminant analysis of principal components: a new method for the analysis of genetically structured populations. BMC Genetics **11**:94. BioMed Central Ltd.

Knutsen H, Jorde PE, Albert OT, Hoelzel AR, Stenseth NC. 2007. Population genetic structure in the North Atlantic Greenland halibut: influenced by oceanic current systems? Can. J. Fish. Aquat. Sci. **64**, 857-866

Legendre P, Fortin M-J. 2010. Comparison of the Mantel test and alternative approaches for detecting complex multivariate relationships in the spatial analysis of genetic data. Molecular Ecology Resources **10**:831–844.

Lotterhos KE, Whitlock MC. 2014. Evaluation of demographic history and neutral parameterization on the performance of FST outlier tests. Molecular Ecology **23**:2178–2192.

Martinez Barrio A et al. 2016. The genetic basis for ecological adaptation of the Atlantic herring revealed by genome sequencing. eLife **5**:311. eLife Sciences Publications Limited.

Marzocchi A, Hirschi JJM, Holliday NP, Cunningham SA, Blaker AT, Coward AC. 2015. The North Atlantic subpolar circulation in an eddy-resolving global ocean model. Journal of Marine Systems **142**:126–143.

Narum SR. 2006. Beyond Bonferroni: Less conservative analyses for conservation genetics. Conservation Genetics **7**:783–787.

Nielsen EE, Hemmer-Hansen J, Poulsen NA, Loeschcke V, Moen T, Johansen T, Mittelholzer C, Taranger G-L, Ogden R, Carvalho GR. 2009. Genomic signatures of local directional selection in a high gene flow marine organism; the Atlantic cod (Gadus morhua). BMC Evolutionary Biology **9**:276.

Oke CS, Ward RD, Crozier RH, Ward RD. 2002. Stock structure of Australian populations of orange roughy analysed using microsatellites. James Cook University, Townsville, QLD, Australia.

O'Leary BC, Brown RL, Johnson DE, von Nordheim H, Ardron J, Packeiser T, Roberts CM. 2012. The first network of marine protected areas (MPSs) in the high seas: the process, the challenges and where next. Marine Policy **36**: 598-605

Ovenden JR, Ovenden JR, Berry O, Berry O, Welch DJ, Welch DJ, Buckworth RC, Buckworth RC, Dichmont CM, Dichmont CM. 2015. Ocean's eleven: a critical evaluation of the role of population, evolutionary and molecular genetics in the management of wild fisheries. Fish and Fisheries **16**:125–159.

Palsbøll PJ, Bérubé M, Allendorf FW. 2007. Identification of management units using population genetic data. Trends in Ecology & Evolution **22**:11–16.

Pante E, Simon Bouhet B. 2013. marmap: A Package for Importing, Plotting and Analyzing Bathymetric and Topographic Data in R. PLoS ONE **8**. Public Library of Science.

R Core Team. 2016. R: A Language and Environment for Statistical Computing.

Reid JL. 1994. On the total geostrophic circulation of the North Atlantic Ocean: Flow patterns, tracers, and transports. Progress in Oceanography **33**:1–92.

Shafer ABA et al. 2015. Genomics and the challenging translation into conservation practice. Trends in Ecology & Evolution **30**:78–87.

Shafer ABA et al. 2016. Reply to Garner et al. Trends in Ecology & Evolution **31**:83–84. Elsevier.

Shephard S, Trueman CN, Rickaby R, Rogan E. 2008. Juvenile life history of NE Atlantic orange roughy from otolith isotopes. Deep-sea Research I 54: 1221-1230.

Spies I, Spencer PD, Punt AE. 2015. Where do we draw the line? A simulation approach for evaluating management of marine fish stocks with isolation-by-distance stock structure. Canadian Journal of Fisheries and Aquatic Sciences **72**:968–982. NRC Research Press.

Upston J, Wayte S. 2012. Orange Roughy (*Hoplostethus atlanticus*) Eastern Zone preliminary stock assessment incorporating data up to 2010 - definition of the base-case model. Pages 180–217 in G. N. Tuck, editor. *Stock Assessment for the Southern and Eastern Scalefish and Shark Fishery 2011. Part 1*. Australian Fisheries Management Authority and CSIRO Marine and Atmospheric Research.

Waples RS. 1998. Separating the wheat from the chaff: patterns of genetic differentiation in high gene flow species. Journal of Heredity **89**:438–450.

Waples RS, Punt AE, Cope JM. 2008. Integrating genetic data into management of marine resources: how can we do it better? Fish and Fisheries **9**:423–449. Blackwell Publishing Ltd. Available from http://dx.doi.org/10.1111/j.1467-2979.2008.00303.x.

Weir BS, Cockerham CC. 1984. Estimating F-statistics for the analysis of population structure. Evolution **38**:1358–1370.

White, T.A., Fotherby, H.A., Stephens, P.A. & Hoelzel, A.R. (2011). Genetic panmixia and demographic dependence across the North Atlantic in the deep-sea fish, blue hake (*Antimora rostrata*). *Heredity* 106, 690–699

White TA, Stamford J, Hoelzel AR. 2010. Local selection and population structure in a deep-sea fish, the roundnose grenadier (Coryphaenoides rupestris). Molecular Ecology **19**:216–226.

White, T.A., Stefanni, S., Stamford, J. & Hoelzel, A.R. (2009). Ocean basin panmixia in a long-lived, deep-sea fish with well-defined habitat dependence and relatively low fecundity. *Molecular Ecology*, 18, 2563-2573.

Table 1. Summary data table, including sampling locations, number of samples per location (*n*), number of polymorphic loci per location (*l*), observed and expected heterozygosity (H_o and H_e, with the inter-quartile range), and inbreeding coefficient (*f*). Source refers to where samples were obtained.

Region	Location	Long	Lat	*n*	*l*	H_o (IQR)	H_e (IQR)	*f* (95% bootstrap CI)	Source
North Atlantic	Bay of Biscay	-2.39	44.66	43	4249	0.3023 (0.1163,0.4419)	0.3212 (0.1312,0.4585)	0.0047 (-0.0019,0.0086)	White et al. 2009
	Faraday Seamount	-28.49	49.48	16	3977	0.2667 (0.1250,0.4375)	0.3167 (0.1208,0.4646)	0.0064 (-0.0004,0.0178)	White et al. 2009
	North Rockall	-9.61	56.17	47	4258	0.3191 (0.1277,0.4468)	0.3256 (0.1312,0.4602)	0.0036 (-0.0014,0.0083)	Francis Neat (Scotland Fisheries)
	Hebrides Seamount	-10.36	56.47	48	4265	0.3125 (0.1250,0.4375)	0.3214 (0.1365,0.4561)	0.0034 (-0.0016,0.0081)	White et al. 2009
	Namibia	13.77	-24.47	58	4423	0.3276 (0.1404,0.4483)	0.3312 (0.1446,0.4561)	0.0064 (0.0001,0.0089)	White et al. 2009
	Porcupine Bank	-14.41	53.79	35	4225	0.3143 (0.1143,0.4571)	0.3244 (0.1345,0.4580)	-0.0013 (-0.0081,0.0034)	White et al. 2009
South Atlantic	Sedlo Bank	-26.91	40.4	50	4248	0.3200 (0.1200,0.4400)	0.3233 (0.1314,0.4592)	0.0025 (-0.0021,0.0073)	White et al. 2009
	South Africa	16.07	-32.93	68	4440	0.3235 (0.1471,0.4412)	0.3295 (0.1497,0.4561)	0.0068 (0.0019,0.0100)	Rob Leslie, David Japp, Melanie Smith (DAFF South Africa, and CapFish)

Table 2. Comparison of *outliers* detect by all four employed methods. Above diagonal: number of loci for which both methods identified as *outliers*; below diagonal: number of loci for which both methods identified as *neutral*; diagonal: number of loci detected as *outlier* by method.

	BayEnv2	**Bayescan**	**Lositan**	**PCAdapt**
BayEnv2	209	54	174	153
Bayescan	3960	64	58	54
Lositan	3863	3892	281	157
PCAdapt	3842	3888	3774	281

Table 3: Pairwise F_{ST} using only the union of neutral loci across all four methods of outlier detection (above diagonal), and using only the union of outlier loci across all four methods of outlier detection (below diagonal). The hypothesis that observed F_{ST} is different from zero was tested with 10,000 bootstraps in Genetix. Significance threshold was corrected for multiple testing to 0.0127. Values highlighted in bold and italics were significantly different from zero. HB – Hebrides; NR – North Rockall; PB – Porcupine Bank; BB – Bay of Biscay; FS – Faraday Seamount; SB – Sedlo Bank; NM – Namibia; SA – South Africa.

	HB	**NR**	**PB**	**BB**	**FS**	**SB**	**NM**	**SA**
HB		-0.00018	0.00046	0.00062	0.00089	0.0007	***0.01037***	***0.01054***
NR	0.00131		0.00016	0.00059	0.00034	-0.00008	***0.01042***	***0.0104***
PB	***0.00378***	***0.00371***		-0.00027	0.00116	***0.00112***	***0.00957***	***0.01031***
BB	0.0005	0.00214	0.00281		0.00184	***0.00197***	***0.00978***	***0.00973***
FS	***0.01546***	***0.01788***	***0.0195***	***0.01601***		0.00022	***0.00966***	***0.01006***
SB	0.00244	***0.003***	***0.00518***	***0.00443***	***0.01424***		***0.01143***	***0.01136***
NM	***0.07289***	***0.07759***	***0.07507***	***0.07224***	***0.09111***	***0.0797***		0.00004
SA	***0.06989***	***0.07575***	***0.07391***	***0.07135***	***0.08743***	***0.07755***	0.0008	

Figure Legends:

Figure 1. Sample distribution across the Atlantic Ocean. NR = North Rockall, HB = Hebrides, PB = Porcupine Bight, FS = Faraday Seamounts, SB = Sedlo Bank, NM = Namibia, SA = South Africa.

Figure 2. BayesScan posterior distribution of F_{ST} relative to a common ancestral population

Figure 3. FCA and DAPC results for both outlier and neutral loci. For outlier loci, we used the union of outlier loci across all four outlier detection methods (420). For neutral loci, we used the union of neutral loci across all four methods.

Figure 4. Regression of genetic distance measured by Euclidean distance between pairwise LD2 DAPC scores to pairwise minimum geographic distance measured along depths between 500 and 2500m. Orange line in part A indicates path within defined depth range.

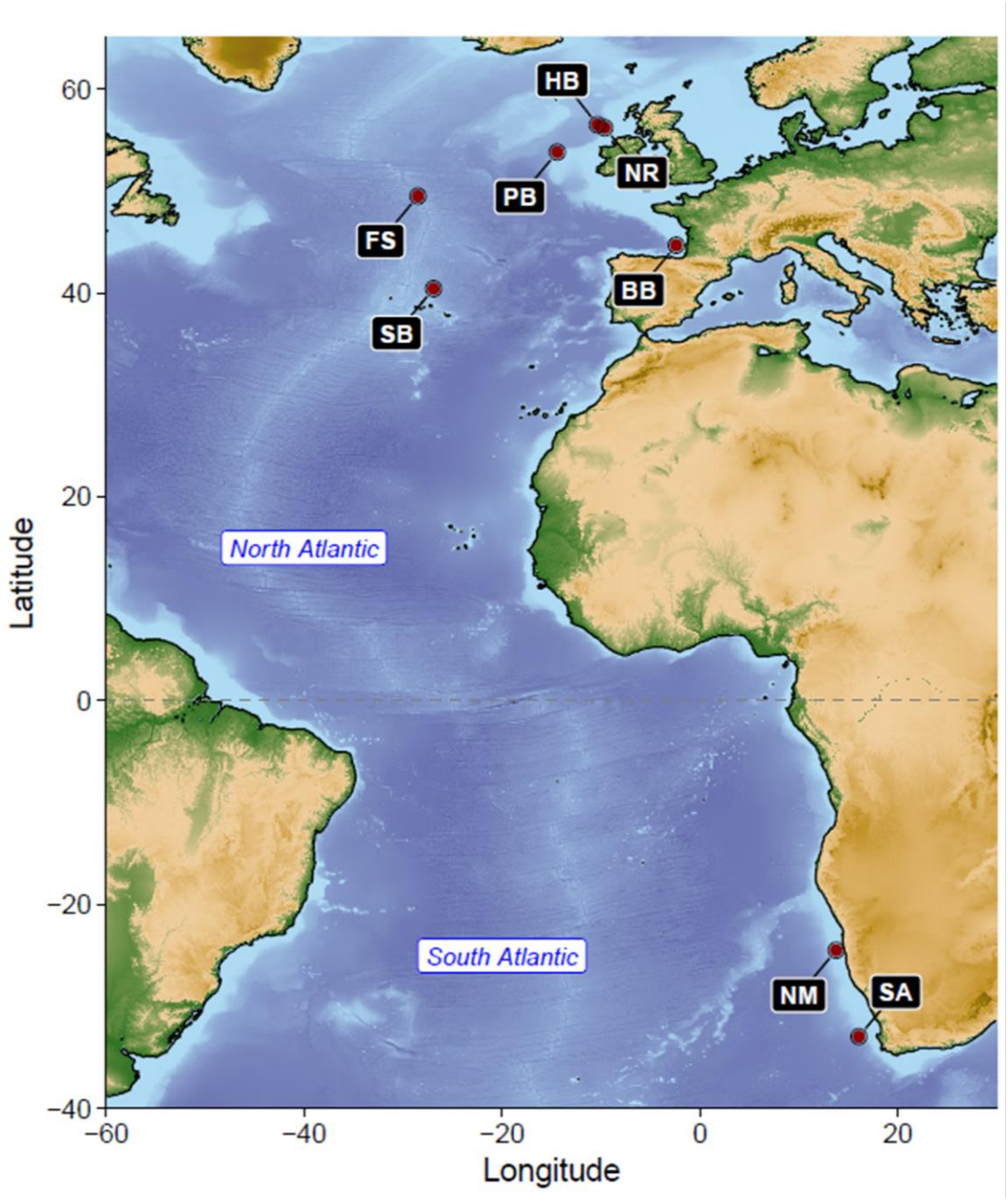
HB
NR
PB
FS
BB
SB
North Atlantic
South Atlantic
NM
SA
60
40
20
0
−20
−40
−60
−40
−20
0
20
Latitude
Longitude

Figure 1.

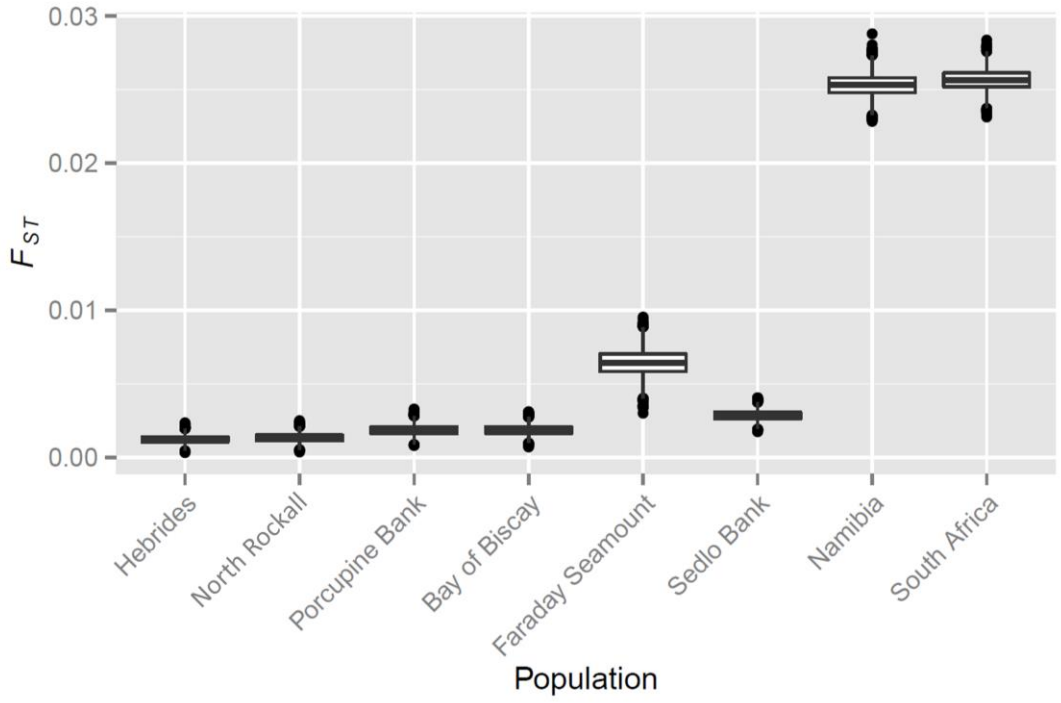
0.03
0.02
0.01
0.00
F_{ST}
Hebrides
North Rockall
Porcupine Bank
Bay of Biscay
Faraday Seamount
Sedlo Bank
Namibia
South Africa
Population

Figure 2.

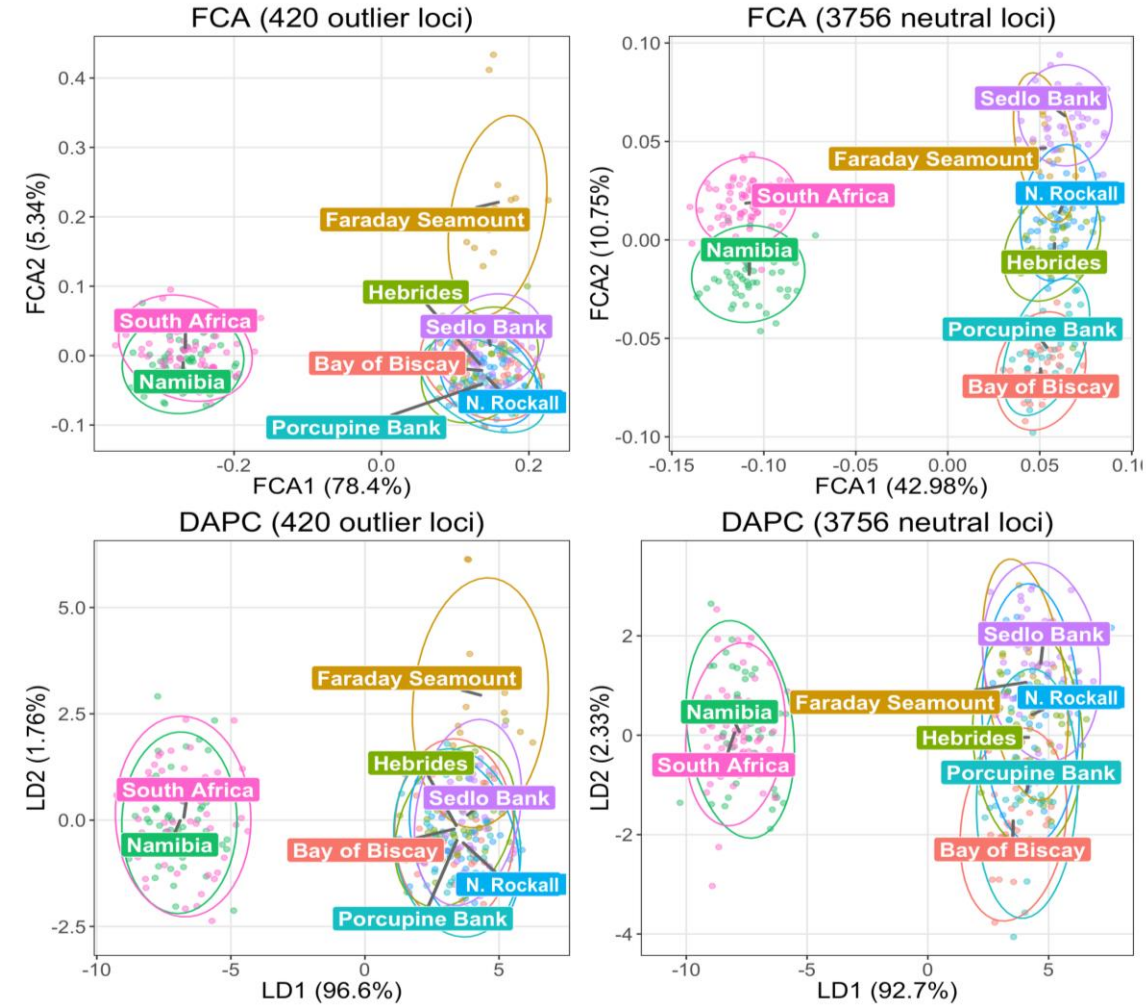
FCA (420 outlier loci)
FCA2 (5.34%)
FCA1 (78.4%)
Faraday Seamount
Hebrides
Sedlo Bank
South Africa
Bay of Biscay
Namibia
N. Rockall
Porcupine Bank
FCA (3756 neutral loci)
FCA2 (10.75%)
FCA1 (42.98%)
Sedlo Bank
Faraday Seamount
South Africa
N. Rockall
Namibia
Hebrides
Porcupine Bank
Bay of Biscay
DAPC (420 outlier loci)
LD2 (1.76%)
LD1 (96.6%)
Faraday Seamount
Hebrides
South Africa
Sedlo Bank
Namibia
Bay of Biscay
N. Rockall
Porcupine Bank
DAPC (3756 neutral loci)
LD2 (2.33%)
LD1 (92.7%)
Sedlo Bank
Namibia
Faraday Seamount
N. Rockall
Hebrides
South Africa
Porcupine Bank
Bay of Biscay

Figure 3.

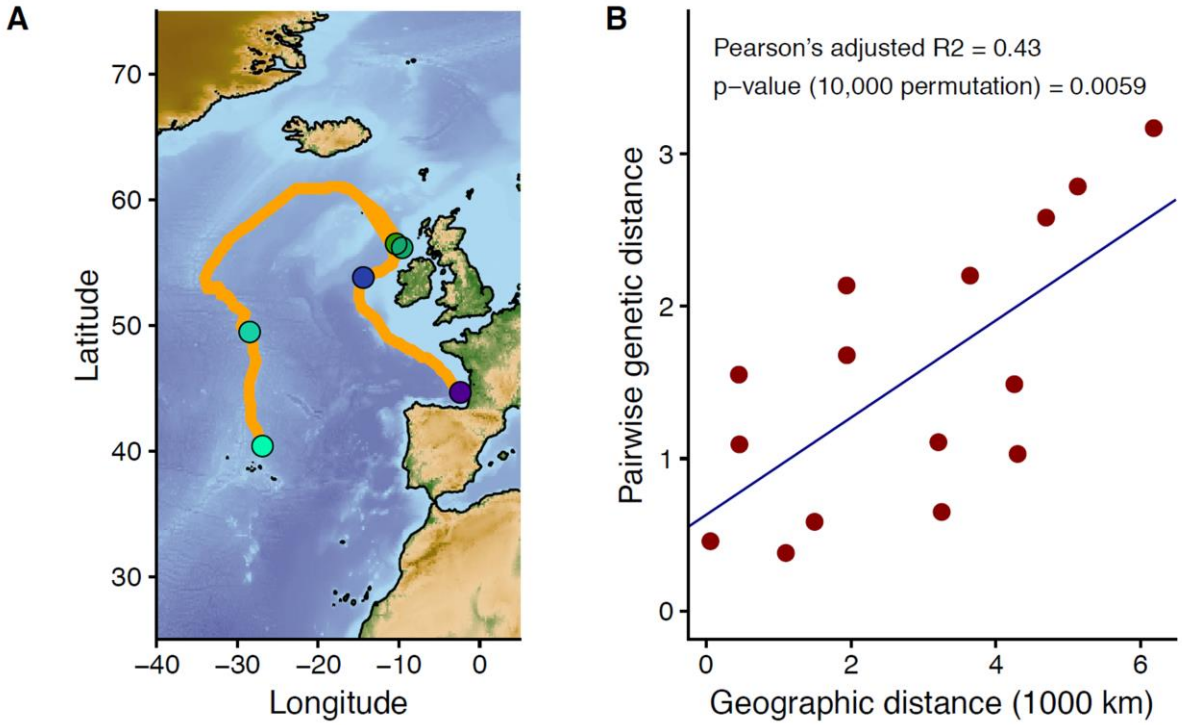
A
70
60
50
40
30
Latitude
−40
−30
−20
−10
0
Longitude
B
Pearson's adjusted R2 = 0.43
p−value (10,000 permutation) = 0.0059
Pairwise genetic distance
3
2
1
0
0
2
4
6
Geographic distance (1000 km)

Figure 4.

Supplementary Information

Quality control of SNP data

Genotyping in GenomeStudio

Using GenomeStudio, we removed all low-quality samples (samples with less than 0.99 genotype calls), we then reclustered the data before filtering out poorly performing loci. Locus quality control followed the manufacturer's recommendations (e.g. removing all loci with a call frequency <0.9993, all loci with repeatability errors, and all monomorphic loci). We then checked individual clusters of SNPs with heterozygote excess or deficiency for abnormal clustering patterns as described in Tindall *et al.* (2010).

Checking LE and HWE, and signatures of ascertainment bias

The resulting 4,567 variable loci across our sample were then tested for linkage equilibrium (LE) and Hardy-Weinberg equilibrium (HWE). For LE, we used the *Bioconductor* package *chopsticks* (Leung 2012) in *R* (R Core Team 2016) to calculate both *D'* and LOD score (log odds ratio of being linked vs. unlinked) for all locus pairs within each sampled location. From the linkage analysis, we identified locus pairs on contigs in linkage disequilibrium and from these created a set of loci with only one randomly chosen locus per contig, yielding 4,179 SNPs. These data have been submitted to the NCBI short read database under accession number XXXXX.

To double check the quality of the set of 4,179 SNPs deemed in LE, we checked for and found no association between call rate and heterozygosity (Figure S1), suggesting that the quality of the samples kept for analyses were largely comparable, and results should reflect true biological differences rather than genotyping artifacts. Finally, the site frequency spectrum across populations and for individual populations did not suggest significant

ascertainment bias, with a roughly 'L'-shaped distribution for loci across populations and within populations (Figures S2 and S3).

Individual locus measures of HWE without regard to population structure were performed and transformed to *z*-scores (with mean 0 and standard deviation 1). Values above the mean suggest heterozygote excess, while values below zero suggest heterozygote deficiency. The distribution has a heavy left tail (Figure S4), which is highlighted in the quantile plot. This suggests a larger number of loci showing heterozygote deficit than expected by the Normal distribution. This is to be expected because: (1) we did not take into account the population structure, which if present, should lead to greater apparent homozygosity; and (2) the SNP site-frequency spectrum is biased towards loci with rare alleles (defined as minor allele frequency < 0.05). A high proportion of such loci have of one allele, which means we should expect to see fewer heterozygotes in the population. These would be harder to sample, and thus to obtain a good estimate of the frequency of heterozygote genotype. In particular, such a frequency bias in the alleles is expected to cause higher sampling variance of the rarer genotypes. An examination of the allele frequency of loci with a z-score < -5 corroborates this assessment (Table S1). Examining the distribution of z-scores within populations suggests a similar skew to that observed across populations (Figure S5). Similarly, the majority of loci showing signs of heterozygote deficiency are loci with rare alleles (Table S2). Thus, for the purposes of the analyses presented here, we consider the set of 4,179 loci proposed to be in LE to also be in HWE.

Identifying outlier loci

Lositan

Outliers were detected in *Lositan* by running the high-capacity version with 50,000 simulations. We selected the options for "neutral" mean F_{ST} and forced mean F_{ST}. Simulations were set to have an expected number of populations of 50, sub-sample size of 50,

and we assumed the infinite alleles mutation model. We then calculated adjusted *p*-values using the Benjamini and Hochberg method (Benjamini & Hochberg 1995), and controlled for a false discovery rate of 0.05. We ran three analyses: (1) with all eight sampled locations, spanning North and South Atlantic; (2) with only the six North Atlantic sampled locations; and (3) with only the two South Atlantic sampled locations. The loci table and the neutral evolution confidence intervals were saved to text files, and plotted in *R* (R Core Team 2016). Based on *p-values* corrected using the Benjamini and Hochberg method (Benjamini & Hochberg 1995), we identified:

- 281 outlier loci across the eight sampling locations (Figure S6A)
- 170 outlier loci across the six sampling locations in the North Atlantic (Figure S6B)
- 47 outlier loci across the two sampling locations in the South Atlantic (Figure S6C)

BayesScan: Convergence

In *BayeScan* 2.1 outliers were detected using the default MCMC parameters across three separate analyses with distinct prior-odds of the neutral model relative to the selection model: 10, 100, and 1000. To assess convergence to the posterior distribution, we plotted individual sample locations chains for the F_{ST} parameter. MCMC was considered to have converged if the chain looked like it was mixing well, as indicated by the characteristic 'caterpillar' look. Loci were deemed outliers if their *q*-value was < 0.01. In each analysis, the prior odds for a model without selection compared to a model with selection was increased by a factor of 10 (range 10 to 1000). The goal was to test prior sensitivity of the results. Otherwise, run conditions were as default. We plotted MCMC chains to visually inspect for convergence to the posterior distribution, and checked the distribution of F_{ST} values (Figure S7).

BayesScan: Identifying outlier loci

We saw an eight-fold decrease in number of identified outlier loci when going from a prior odds of 10 to a prior odds of 1000 (64 vs 8 outlier loci; Figure S8). The median posterior probability of a locus identified as an outlier being a true outlier increased from 0.79 to 0.85 across the different priors (Figure S9).

PCAdapt: Determining the number of factor, K

PCAdapt (version 1.5) attempts to jointly estimate population structure and identify loci that are disproportionately associated with structure (outliers) (Duforet-Frebourg *et al.* 2014). The number of factors, *K*, is an unknown parameter of the *PCAdapt* model. The authors discuss different heuristics in order to determine the optimal *K* (Duforet-Frebourg *et al.* 2014). In our analysis, we determined *K* by first exploring the decay of MSE with increasing *K*, with *K* ranging from 1 to 12. To obtain MSE estimates, the model was run 10 times for each *K*. To check for convergence of the MCMC, we followed the authors suggestion to calculate the correlation among independent runs of the MCMC for each *K* (where high correlation is suggestive of convergence and good results) We found high correlation for $K = 1$ ($R^2 \sim 1$), and low correlation for subsequent *K* values. We ran both available models with the raw count matrix as input, and a random start to the MCMC, and with a singular value decomposition (SVD) of the input matrix. The results for each model both suggested that the optimal $K = 1$. In Figure S10, we show results for the model not initialized with SVD and without a scaled *Y* input vector.

PCAdapt: Choosing outlier loci

For each locus *PCAdapt* calculates an approximation of the log_{10} (Bayes Factor), which indicates how much more likely the locus data fits a model in which the locus is an outlier relative to a model where it is not an outlier (Figure S11). For convenience of

comparison to traditional *log* Bayes Factor scales, we have transformed the values into natural *log* scale, which henceforth we refer to as *lnBF*. There is no simple heuristic that we can specify *a priori* that allows us to be certain of the FDR given a *lnBF* threshold of significance (Duforet-Frebourg *et al.* 2014). We therefore took a multiple approach in order to classify loci as outliers. First, based on the scale of Kass and Raftery (1995) we identified all loci that had a $2 \times lnBF \geq 6$ (considered to be strong evidence against the *null* model that the locus is not an outlier). Here, *lnBF* was taken as the mean *lnBF* across 10 replicate runs. For these loci, we examined the strength of association between the loci and the factor to satisfy ourselves that there is indeed an appreciable effect. In total, we identified 281 outlier loci with *PCAdapt*.

BayEnv2: Checking for convergence

Using *BayEnv2* (Günther & Coop 2013) we estimated the degree of association between each of the 4,179 SNPs to North or South Atlantic across each of 50 random posterior covariance matrices (five from each of the replicate chains). The estimate of association for each SNP x covariance matrix pair was performed with an MCMC of 500,000 steps. Thus, for each SNP, we had 50 estimates of Bayes Factor of association, and 50 estimates of Spearman's ρ and Pearson's r_s. We first ran 50 replicate MCMC to estimate the among population SNP covariance matrix. From each replicate run we drew 1000 samples, recorded every 500^{th} step, and discarded the first 500 as burn-in. To examine convergence, we plotted the chain for each element of the 8 x 8 covariance matrix (Figure S12).

BayEnv2: Identifying outlier loci

As noted by Coop *et al*. (2010), there can be large variation in estimates of Bayes Factors for single loci with different priors and across loci, and a large Bayes Factor is no guarantee of an association between a SNP and an environmental variable. The authors

recommend building an empirical distribution of Bayes Factors from control SNPs in order to identify significant Bayes Factors. In lieu of control SNPs, we used the distribution of minimum Bayes Factors across the 50 estimates for each locus, and set the threshold of minimum Bayes Factor at the top 5% of Bayes Factors observed. The identified threshold was 4.52. To ensure our heuristic was working, we searched for associations between Bayes Factors and Spearman's ρ and Pearson's r_s in order to identify outlier loci (Figure S13). In total, we identified 209 outlier loci with *BayEnv2*. The numbers of outliers identified by the various methods is illustrated in a Venn diagram in Figure 2.

Outlier loci detected

Using Lositan we identified 281 outlier loci out of the 4179 loci included in the analysis across all eight sampling locations after adjusting for false discovery. This was reduced to 170 when considering only the sampling locations in the North Atlantic, and 47 when examining only the South Atlantic sampling locations (Figure S6). To quantify the difference between outlier and neutral loci, we compared the F_{ST} values between both sets of loci. We found a strong effect distinguishing outlier from neutral loci when all populations were included, with mean F_{ST} of outlier loci being an order of magnitude greater than that of neutral loci (mean outlier F_{ST} = 0.049; mean neutral F_{ST} = 0.0059; Student's *t*-test: t = 47.281, df = 298.65, p-value < 2.2e-16). Mean heterozygosity of outlier loci was also significantly greater than that of the neutral loci (mean outlier heterozygosity = 0.337; mean neutral heterozygosity = 0.301; Student's *t*-test: t = 3.99, df = 333.58, p-value = 7.8e-5). A similar pattern was observed for the analysis including only samples from the North Atlantic (mean outlier F_{ST} = 0.035; mean neutral F_{ST} = 0.0077; Student's *t*-test: t = 30.91, df = 179.19, p-value < 2.2e-16; mean outlier heterozygosity = 0.338; mean *neutral* heterozygosity = 0.297; Student's *t*-test: t = 3.56, df = 216.33, p-value < 0.0005). Given the expectation (and

empirical record) of marine species (including orange roughy) having high connectivity and low F_{ST}, this difference supports the interpretation of selection, but is not conclusive.

For *BayesScan*, visual inspection of the MCMC for the F_{ST} parameter suggested convergence to the posterior distribution in all three analyses (Figures S7 & S9). Our analysis identified 64, 19, and 8 *outlier* loci when setting the prior odds of a neutral model in relation to a model with selection to 10, 100, and 1000, respectively (Figure S8), and using a *q*-value of 0.05, which sets the FDR to 5%.

The locus effect in *BayesScan* (α) reflects selection and locus specific mutation rates (Beaumont & Balding 2004). The median α across the three prior treatments was close to zero for loci classified as outliers, and 1.37, 1.55, and 1.72 for prior odds of 10, 100, and 1000, respectively. This suggests that, at least in terms of locus specific effects, at neutral loci the probability that two alleles taken at random from a population are just as likely to have a common ancestor within the sampled population as they are to not have a common ancestor in the population. For outlier loci the probability increases to 0.80, 0.82, and 0.84 for the each of the three prior treatments, respectively.

For *PCAdapt*, the most likely number of splits (*K*) was one. We inspected both the decay of MSE and the correlation among runs of the association of loci to factors across multiple MCMC strategies. We did not observe the expected plateau in MSE unless we started the MCMC with an SVD input matrix. The correlation between loci and assigned factors between runs across all approaches had $r^2 > 0.95$ only for $K = 1$. Plots of $K = 1$ separate samples from North and South Atlantic (Figure S10), while $K \geq 2$ do not indicate any clear structure.

A total of 281 loci were found to be outliers with our criteria of $2 \times lnBF \geq 6$. The *lnBF* ranged from 0.91 to 18.49 across all loci and 10 replicate runs. Mean values across

replicate runs for individual loci ranged from 1.25 to 18.30. The standard deviation across replicates was only slightly associated with mean *lnBF* (R^2 = 0.25; Supplementary material).

The effect size, measured by correlation between loci and factors, was generally small. A negative association means that the most common allele in the North Atlantic was the minor allele in the South Atlantic, and the converse applies to a positive association (Figure S11). The strength of association between loci and factors ranged from -0.11 to 0.08, with mean = 0 (±0.02). The range of correlation values for non-outlier loci was between -0.036 to 0.036, with mean = 0 (±0.015).

The number of outlier loci was reduced to 48 (18 with a positive *r*, and 30 with a negative *r*) by focusing only on the loci that had an *r* value at least 1.5X larger than the minimum or maximum *r* value observed for those loci deemed neutral. The value of 1.5X was arbitrarily chosen to be about half the maximum fold difference in *r* value between neutral and outlier loci observed across the dataset (3.12X).

For *BayEnv2* the length of the individual MCMC for estimation of the posterior distribution of covariance matrices was suitable, as suggested by the plot of the individual element chains (Figure S12). A plot of the mean covariance matrix suggests significant differences between the North and South Atlantic. Within each ocean, population allele frequencies have positive covariances. However, Faraday Seamount seems to show allele frequencies that are distinct from those of other sampled locations in the North Atlantic.

Estimates of Bayes Factors (BF) ranged from 7.12×10^{-2} to 7.83×10^{5}. Taking just the minimum BF for each SNP across the 50 posterior samples, the values ranged from 7.12×10^{-2} to 3.17×10^{3}. The 95th quantile of the minimum BF values was ~4.53, and all loci with minimum BF value equal to or above the 95th quantile were labelled as outliers, resulting in 209 outlier loci. The distribution of absolute values of Pearson's r_s coefficient and Spearman's ρ were similar for outlier and neutral loci (results for Pearson's r_s for neutral loci

were median = 0.18 with 2.5% and 97.5% quantiles equal to 0.008 and 0.48, respectively; for *outlier* loci median = 0.44 with 2.5% and 97.5% quantiles equal to 0.23 and 0.63, respectively; Figure S13). Shared outlier loci among methods is shown in Figure S14, while Figure S15 shows support for similar outlier patterns in FCA for methods run separately. Figure S16 shows the contribution of the number of loci to the resolution of the analysis.

References

Benjamini Y, Hochberg Y (1995) Controlling the False Discovery Rate - a Practical and Powerful Approach to Multiple Testing. *Journal of the Royal Statistical Society Series B-Methodological*, **57**, 289–300.

Coop G, Witonsky D, Di Rienzo A, Pritchard JK (2010) Using environmental correlations to identify loci underlying local adaptation. *Genetics*, **185**, 1411–1423.

Duforet-Frebourg N, Bazin E, Blum MGB (2014) Genome scans for detecting footprints of local adaptation using a Bayesian factor model. *Molecular Biology and Evolution*, **31**, msu182–2495.

Kass R, Raftery AE (1995) Bayes Factors. *Journal of the American Statistical Association*, **90**, 773–795.

Leung H-T (2012) *chopsticks: The snp.matrix and X.snp.matrix classes*.

Tindall EA, Petersen DC, Nikolaysen S *et al.* (2010) Interpretation of custom designed Illumina genotype cluster plots for targeted association studies and next-generation sequence validation. *BMC Research Notes*, **3**, 39.

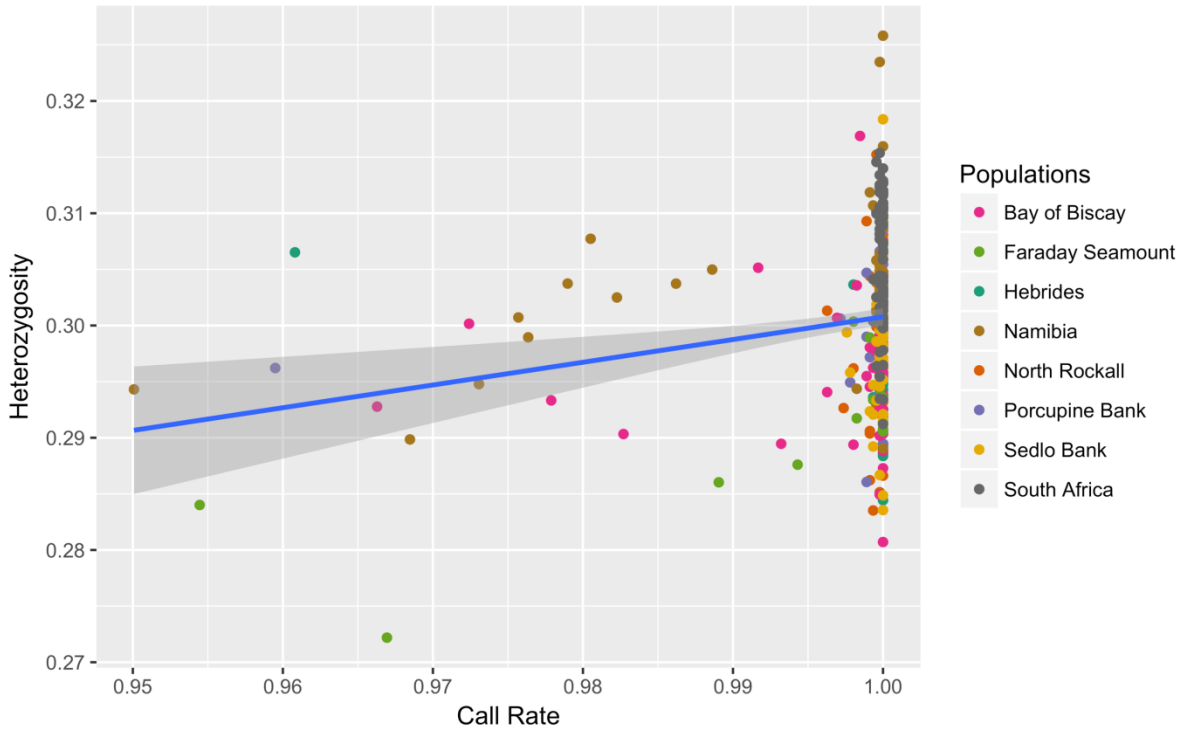

Figure S1. Distribution of genotyping call rate vs heterozygosity (Adjusted R^2 = 0.03)

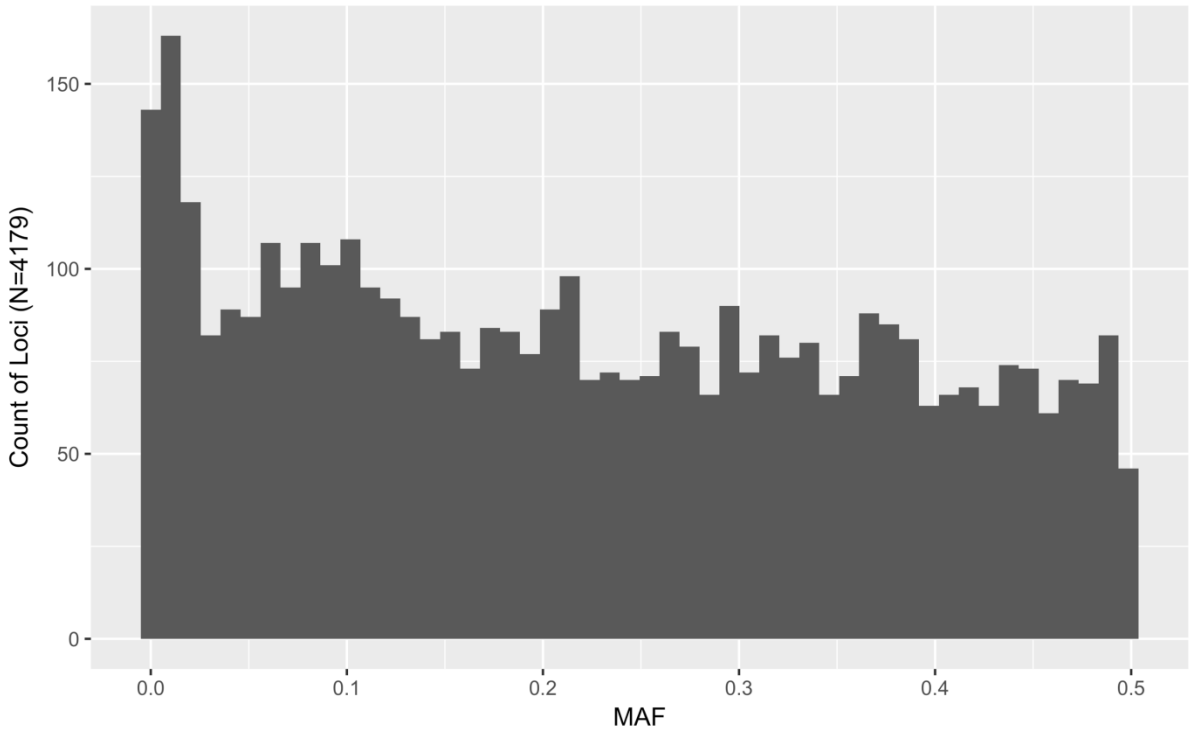

Figure S2. Site frequency spectrum of 4,179 SNPs of orange roughy samples from the Atlantic Ocean

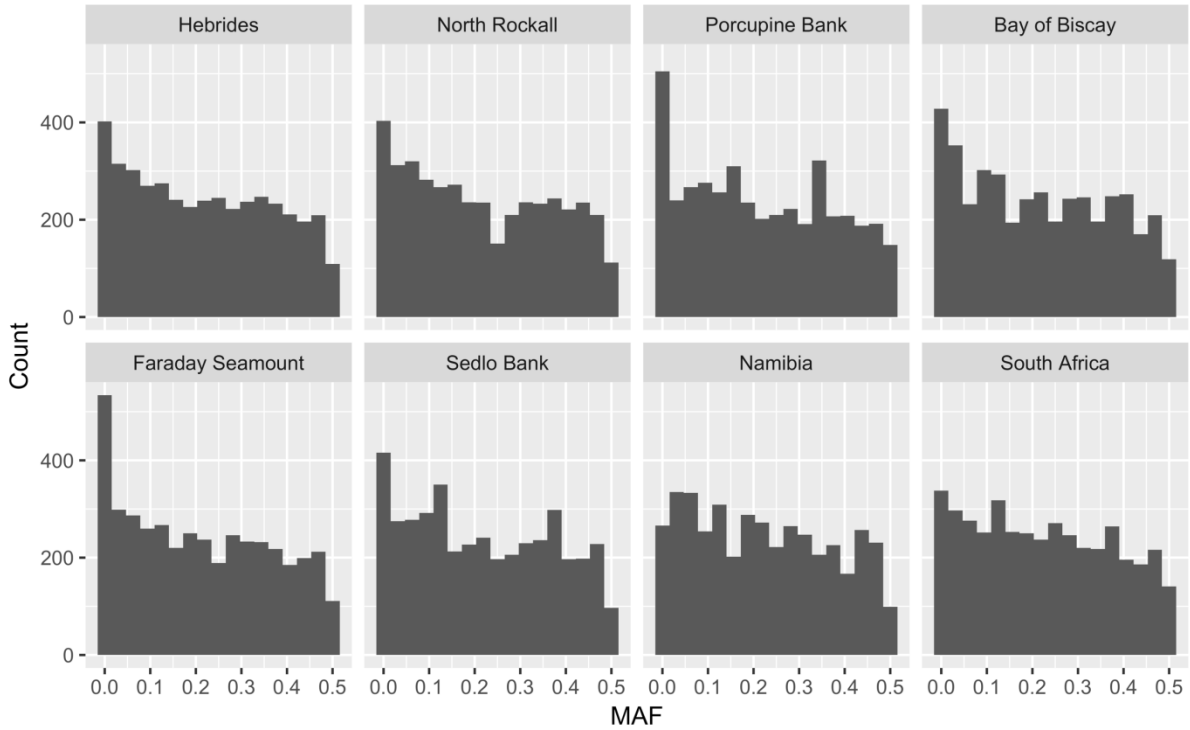

Figure S3. Site frequency spectrum of 4,179 SNPs of orange roughy samples from eight sampling locations in the Atlantic Ocean

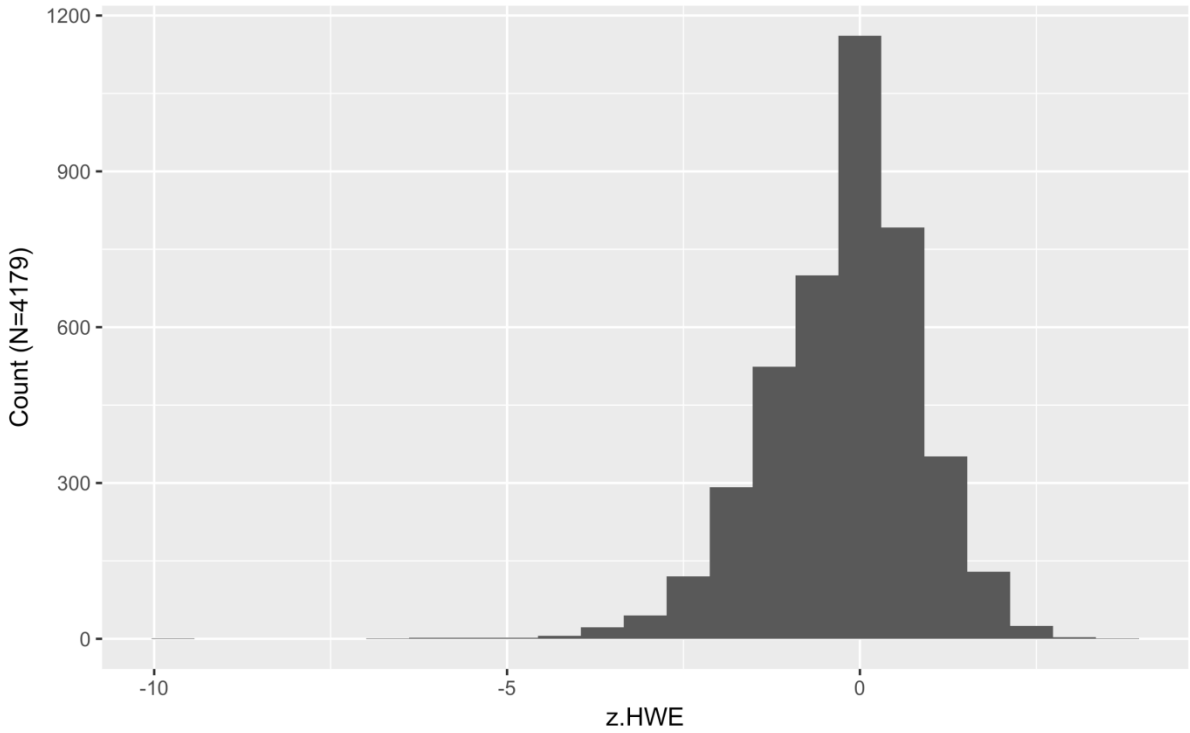

Figure S4. Distribution of *z* scores (deviations from expected genotypic frequencies given allelic frequencies) across all 4,179 SNPs in the sample of 365 orange roughy from the Atlantic Ocean

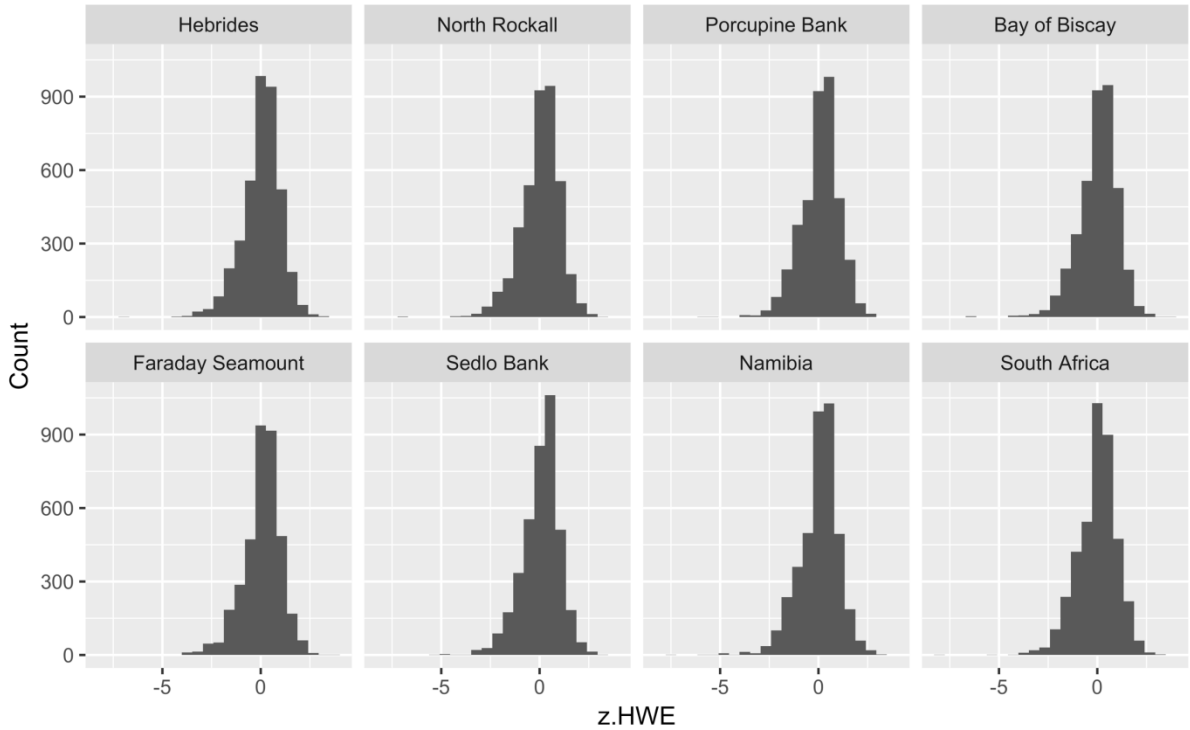

Figure S5. Distribution of *z* scores (deviations from expected genotypic frequencies given allelic frequencies) across all 4,179 SNPs in the sample of 365 orange roughy from the Atlantic Ocean for each of eight sampling locations

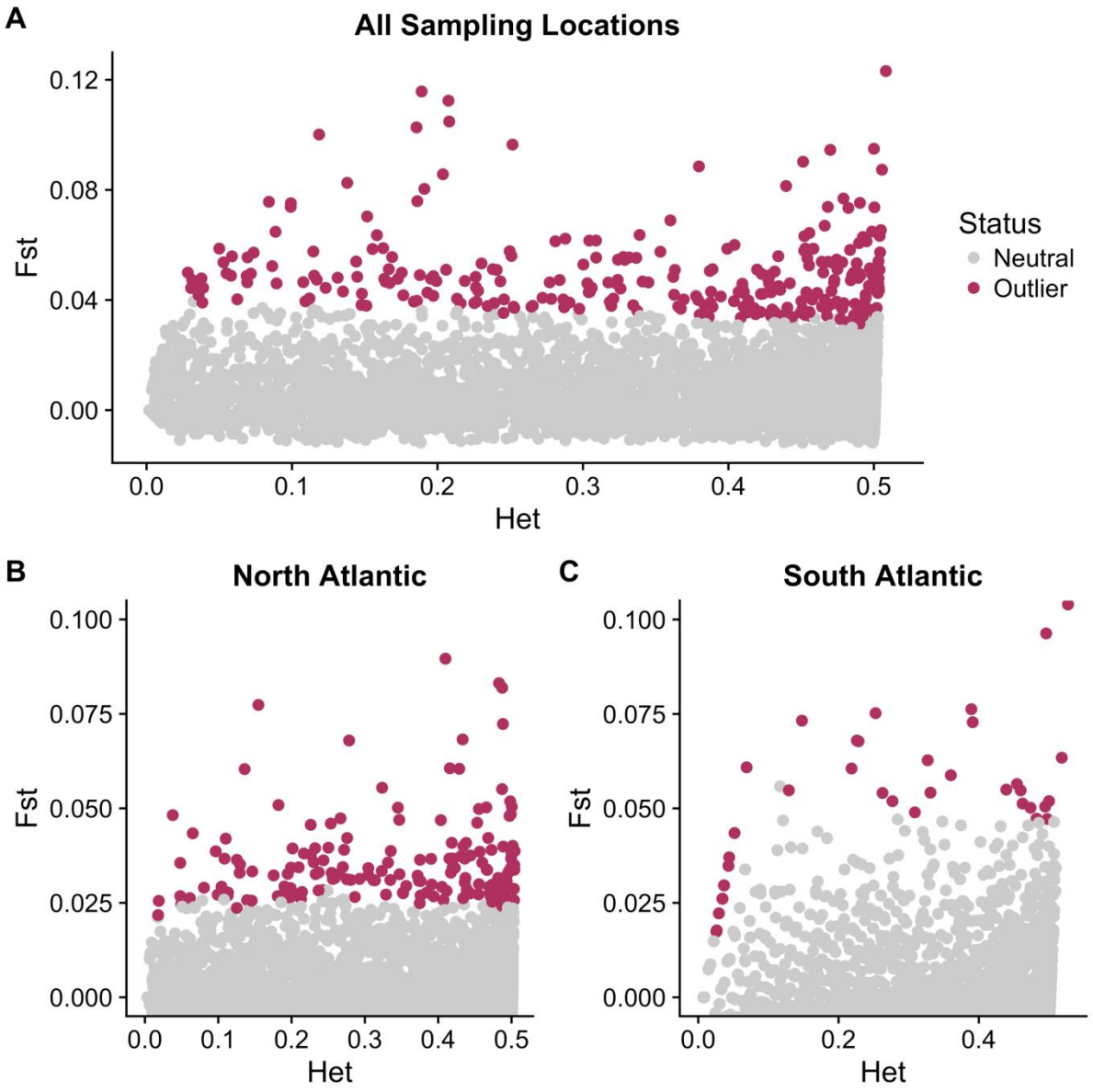

Figure S6. Distribution of outlier and neutral loci as identified using Lositan. Outlier loci were defined as those with an adjusted *p*-value ≤ 0.05.

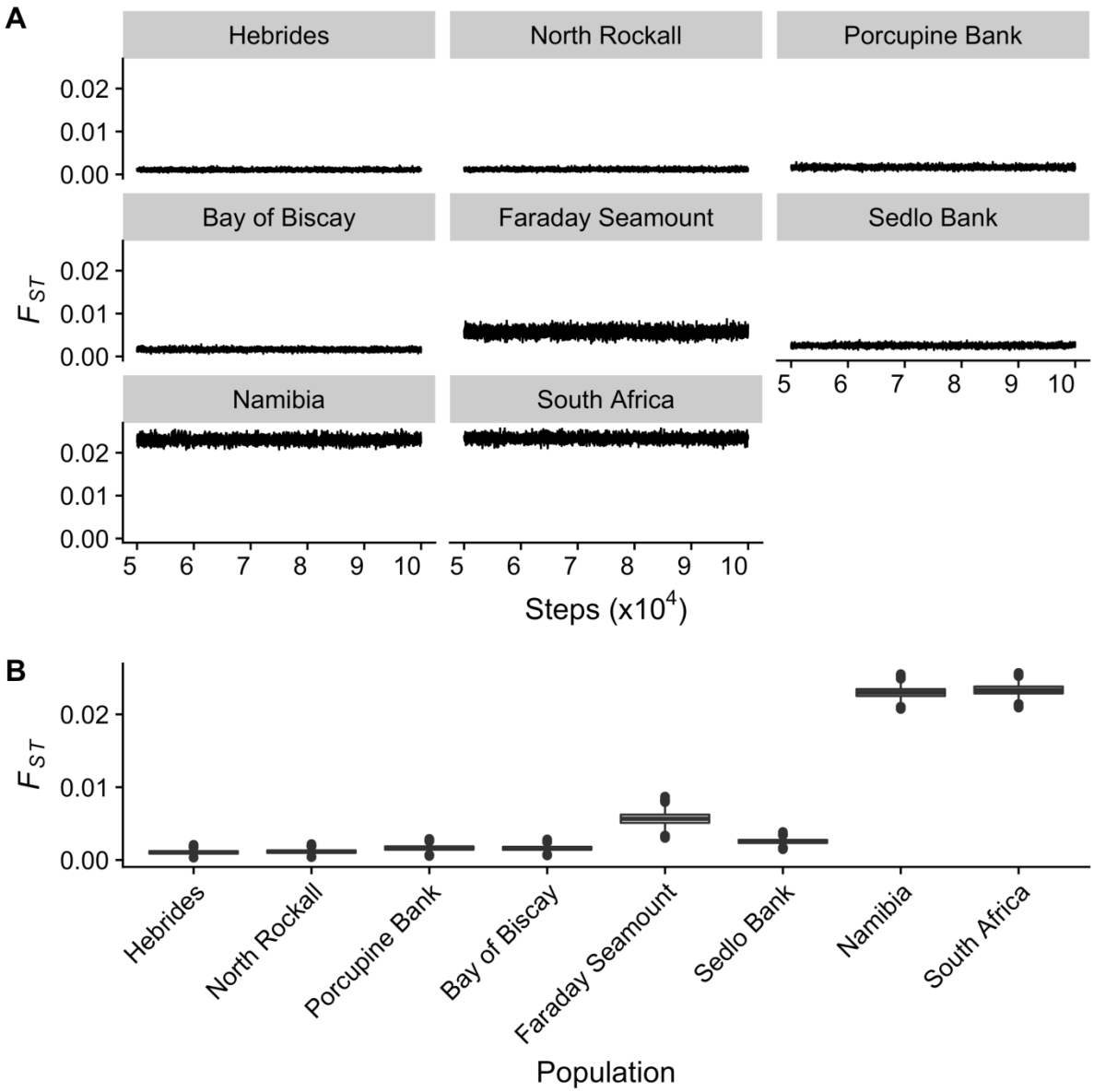

Figure S7. BayesScan 2.1 MCMC output assuming a prior odds of 10:1 of the neutral model relative to the selection model. A. Plots of MCMC demonstrating convergence to stationarity. B. Posterior distribution of BayesScan FST values.

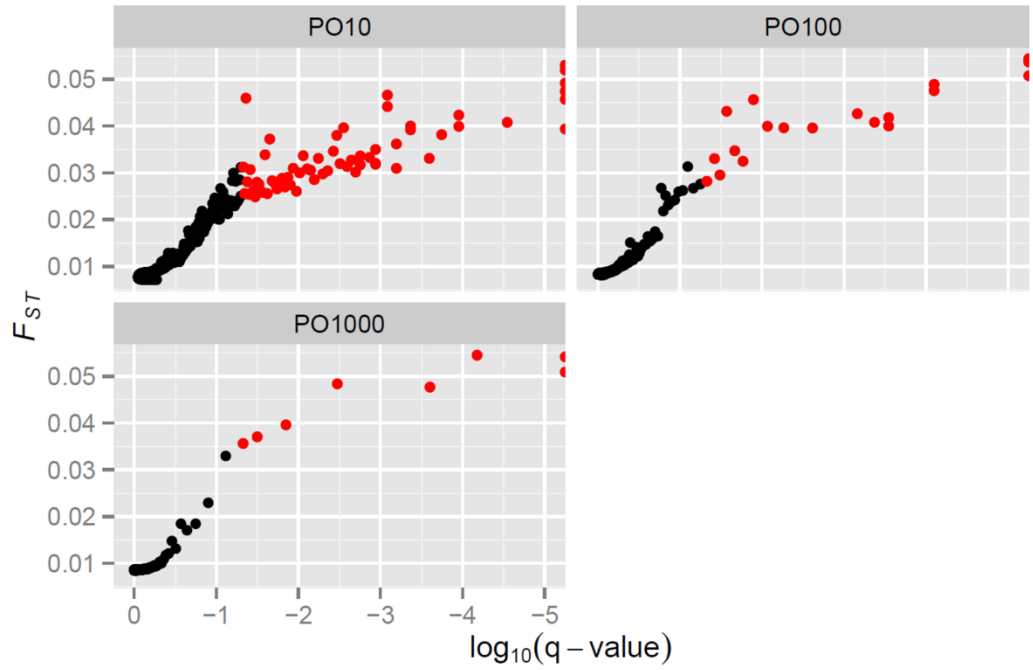

Figure S8: Identification of outlier loci across runs of BayeScan with different prior odds (PO) on model with (shaded dots to the right) and without (shaded dots to the left) selection.

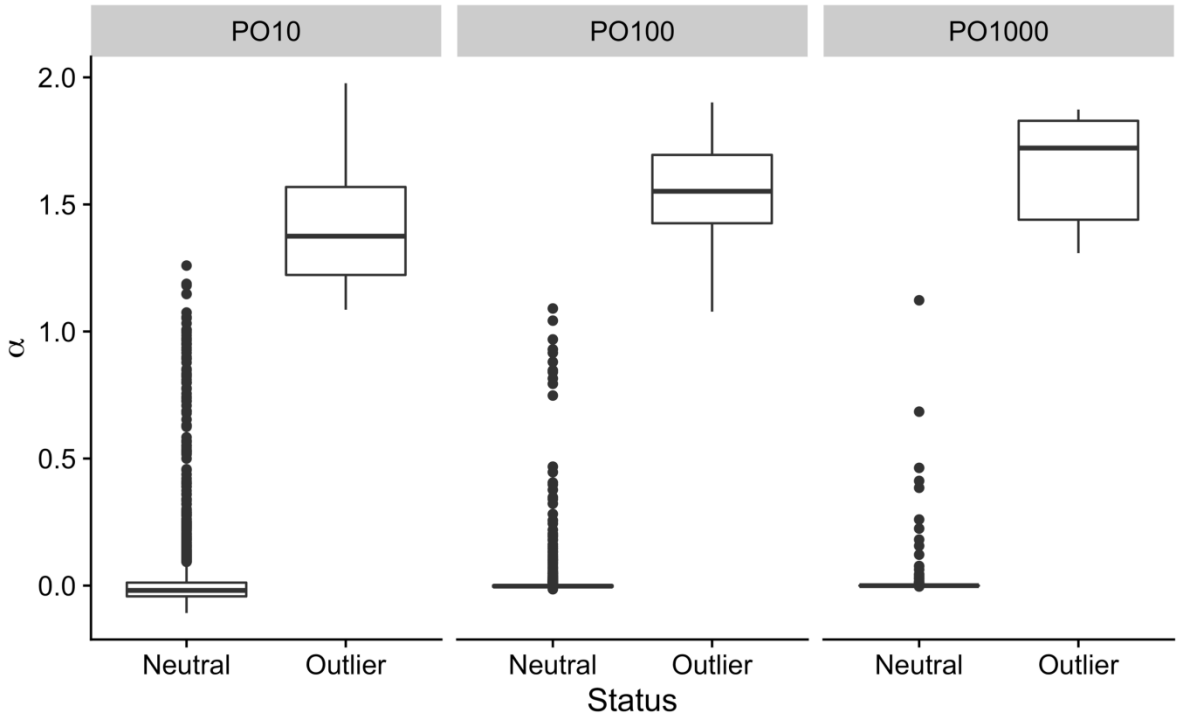

Figure S9. Distribution of α for neutral and outlier loci across the three prior treatments

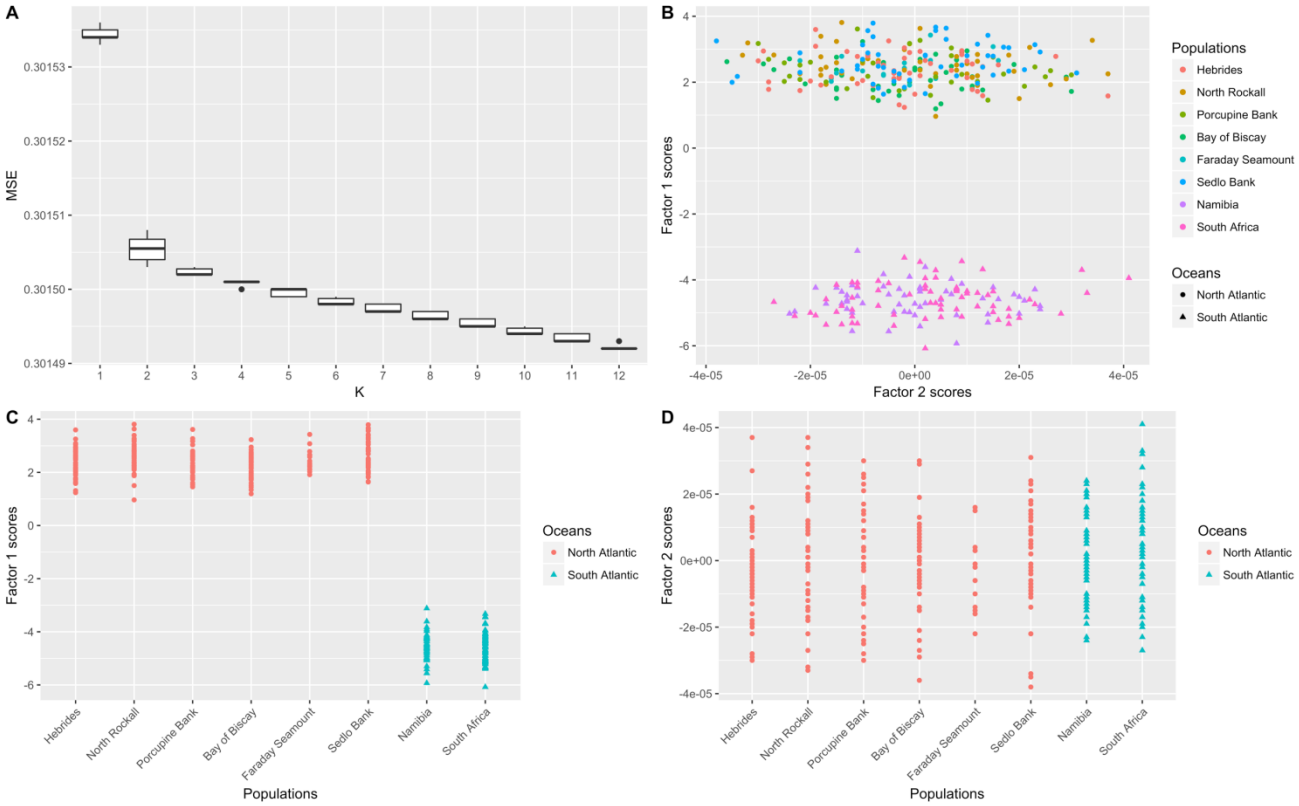

Figure S10. Determining optimal number of factors, *K*, for PCAdapt. A. Mean squared error against *K*, suggesting *K* = 1 is best; B. Scores of Factor 1 against Factor 2 scores showing that only Factor 1 discriminates between North and South Atlantic; C. Distribution of Factor 1 scores across sampling locations; D. Distribution of Factor 2 scores across sampling locations.

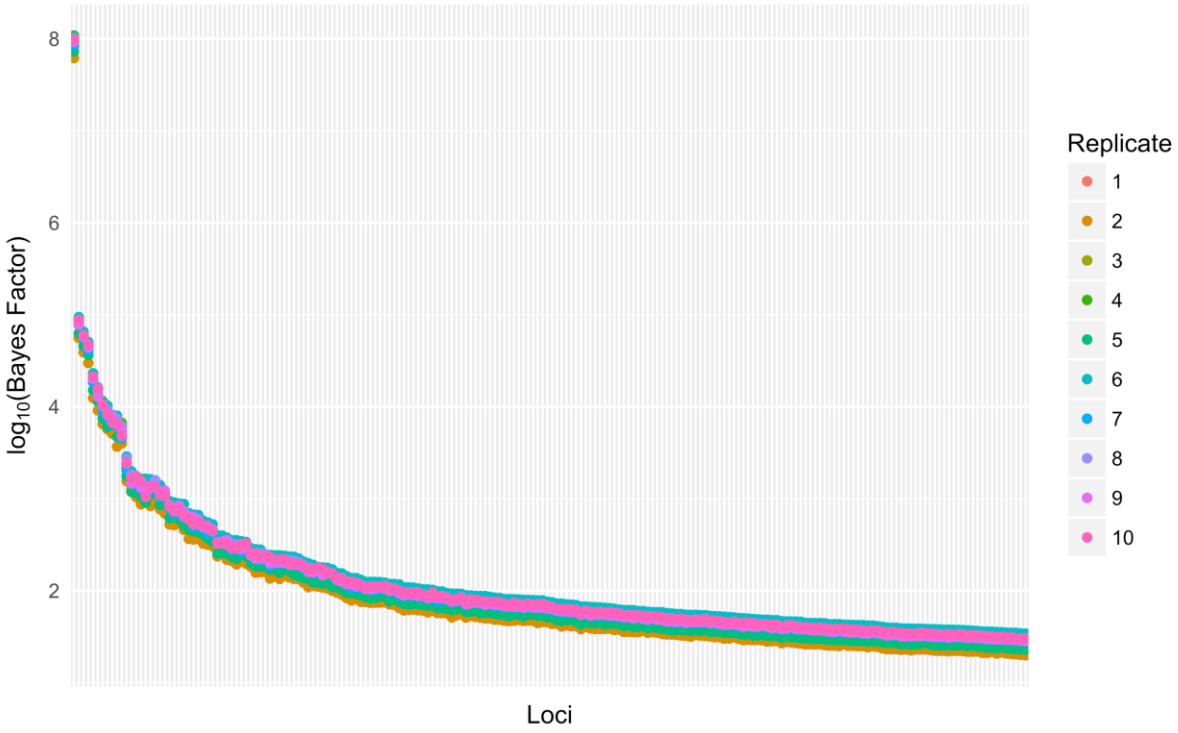

Figure S11. Distribution of log Bayes Factor across 10 replicate runs of PCAdapt for all 4,179 loci

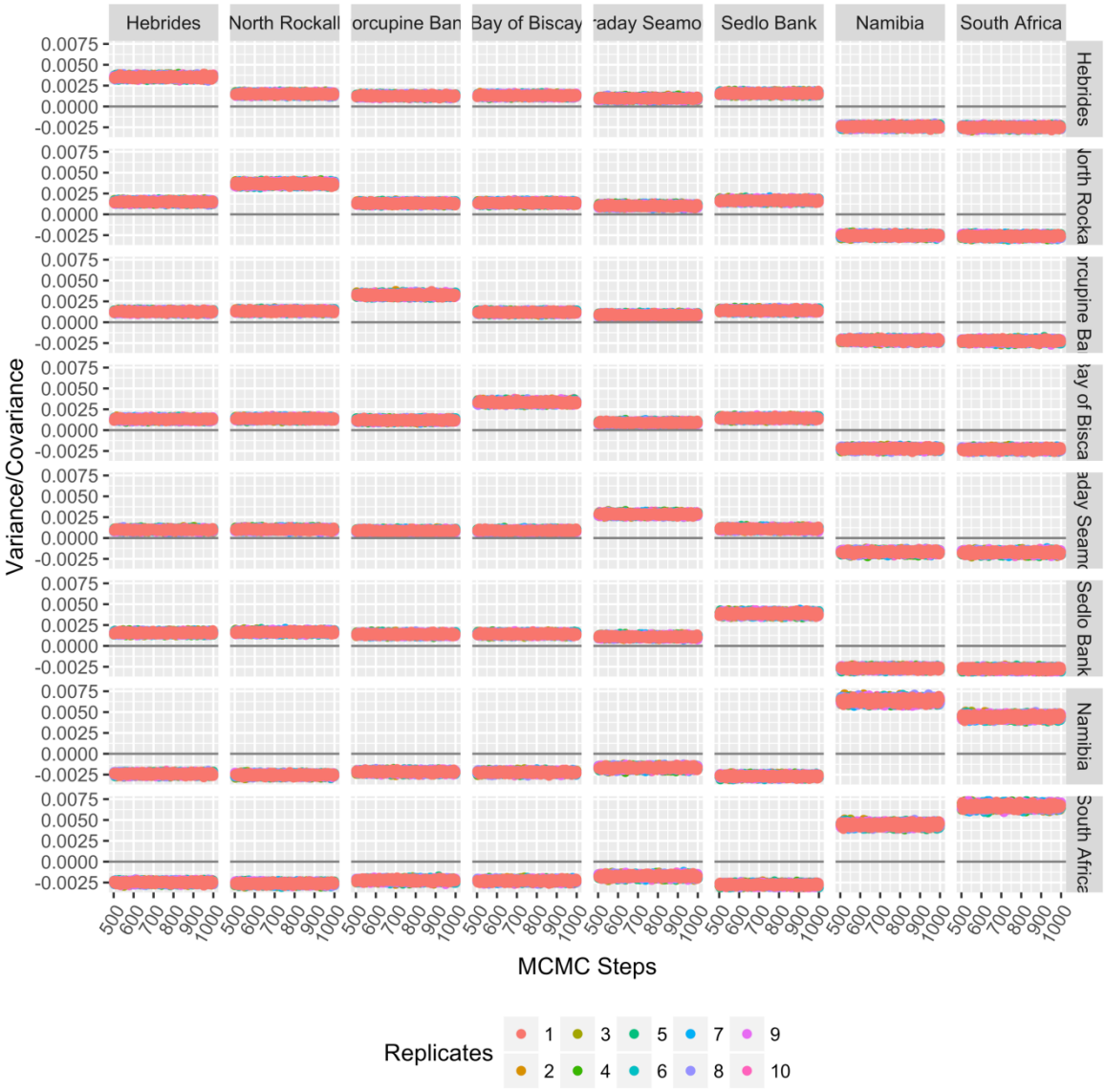

Figure S12. *BayEnv2* MCMC samples of the posterior distribution of the covariance matrix. Plots includes samples taken across 10 independent runs, and only display samples taken after burn-in. For each run, 500 samples were recorded after burnin, taken every 500th step.

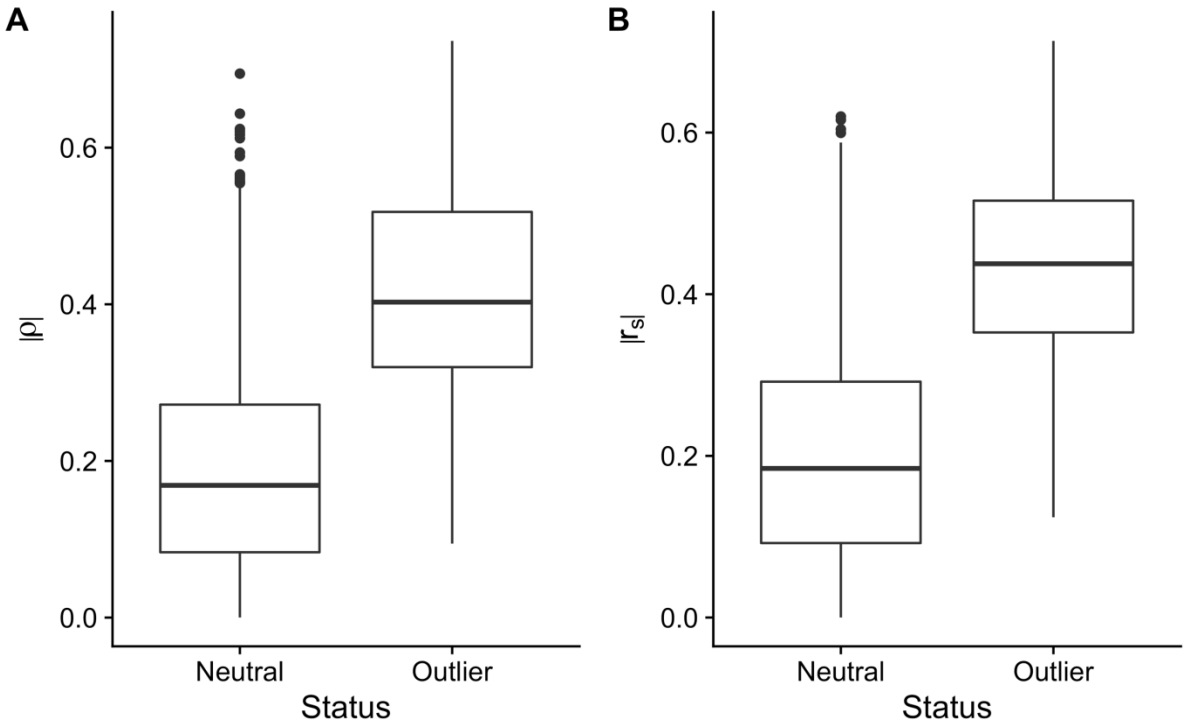

Figure S13. Distribution for neutral and outlier loci of absolute values of: (A) Spearman's Rank ρ scores across Bayes Factors; (B) Pearson's Correlation Coefficient r_s scores

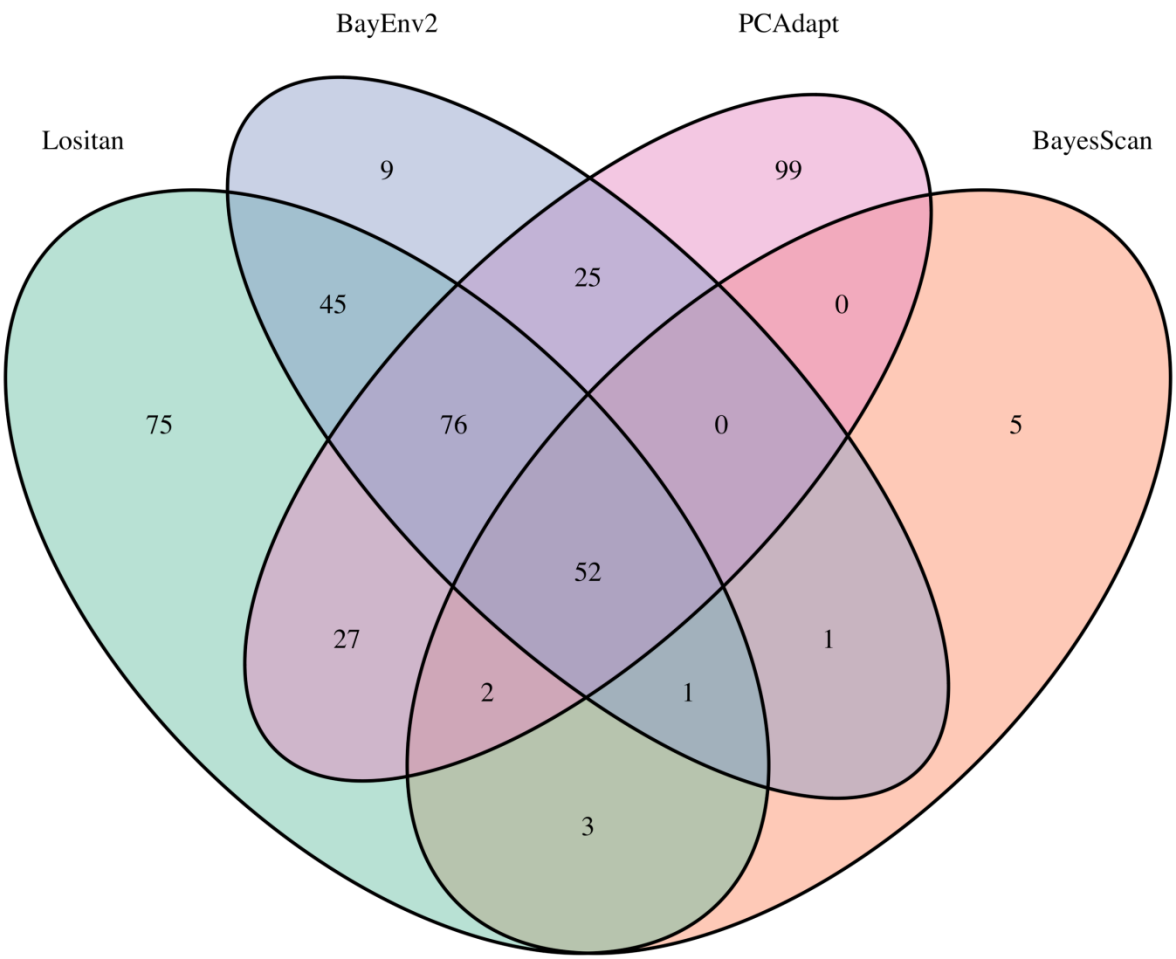

Figure S14. Venn diagram of count of shared outlier loci across outlier detection methods

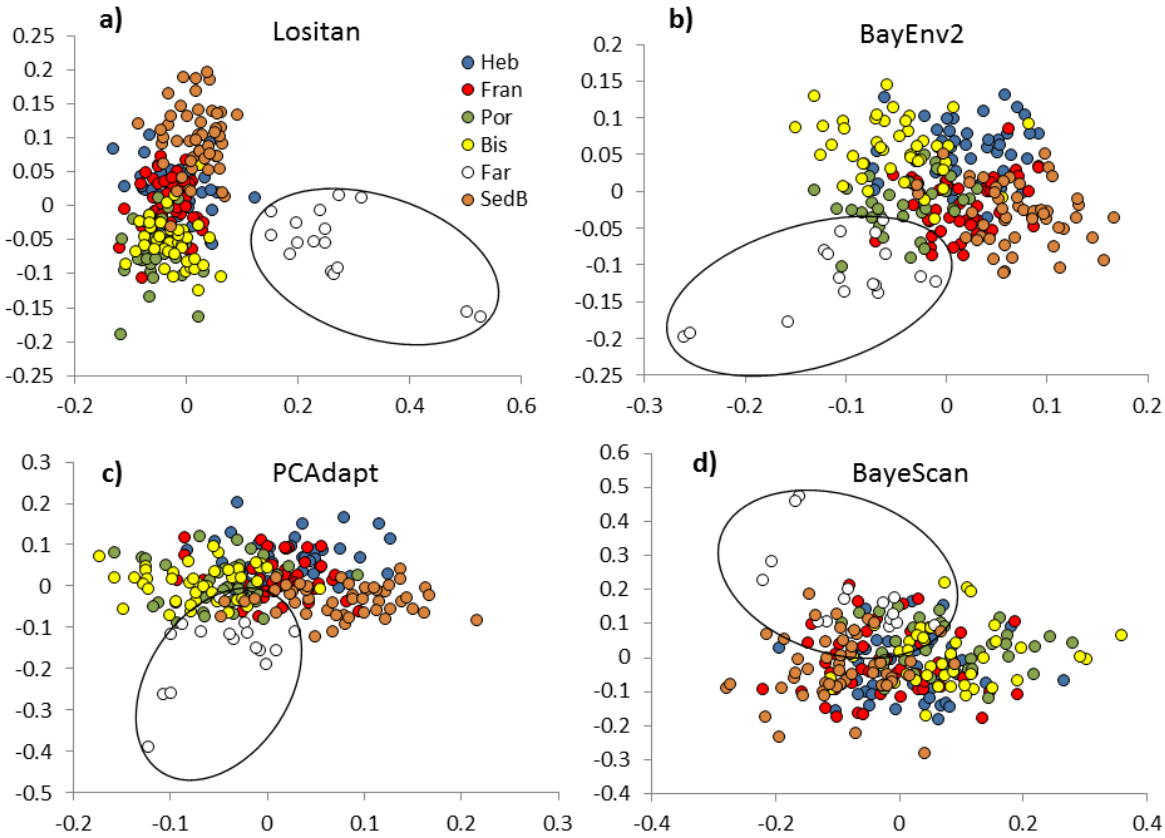

Figure S15: FCA analysis of a) 281 outlier loci from the Lositan analysis; x-axis: factor 1 (32.5%), y-axis: factor 2 (20.1%). b) 209 outlier loci from the BayEnv2 analysis; x-axis: factor 1 (23.8%), y-axis: factor 2 (23.3%). c) 281 outlier loci from the PCAdapt analysis; x-axis: factor 1 (23.1%), y-axis: factor 3 (20.7%). d) 64 outlier loci from the BayeScan analysis; x-axis: factor 1 (30.3%), y-axis: factor 3 (20.1%). The Faraday population is circled in all panels. Note that factors 2 and 3 had essentially the same support in all cases, and so the most informative pairing with factor 1 is illustrated.

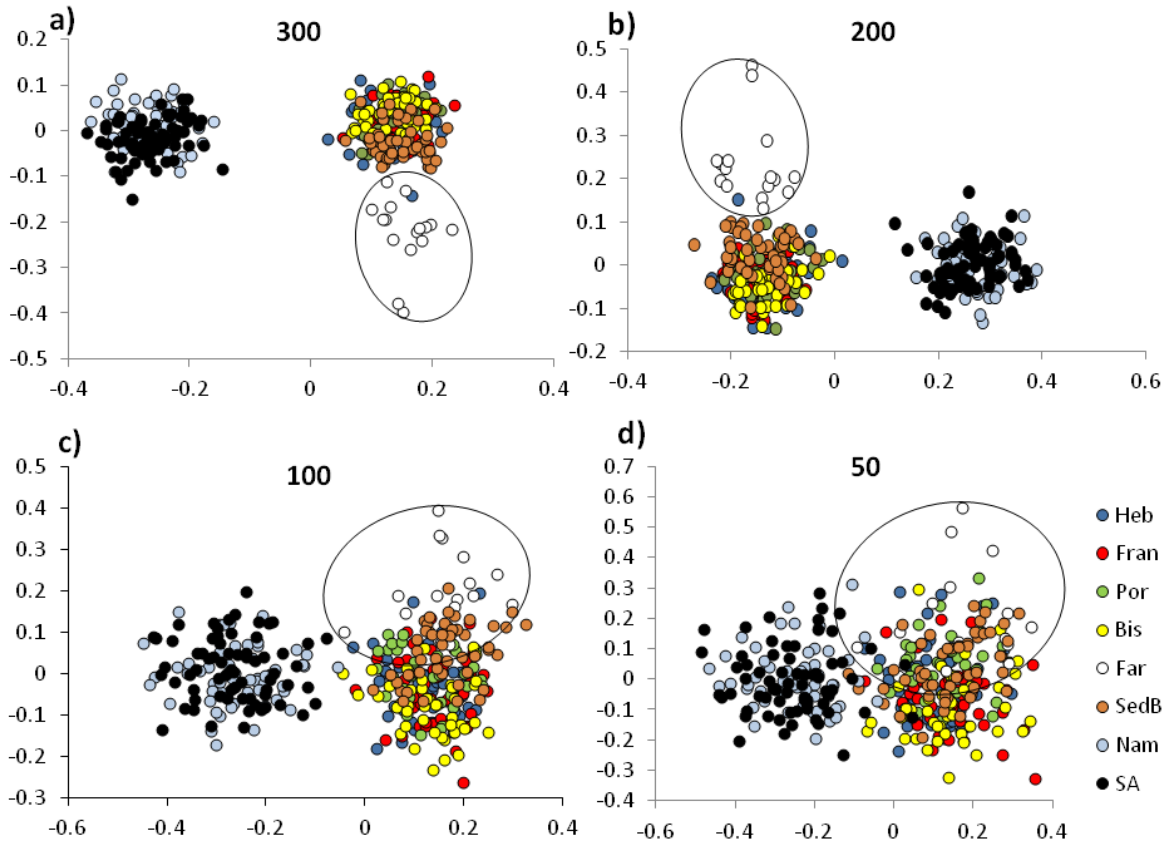

Figure S16: Test FCA analyses based on random subsamples of loci from the total of 420 combined from all four analytical methods (Lositan, Bayscan, BayEnv2 and PCAdapt). a) 300 loci, b) 200 loci, c) 100 loci, d) 50 loci. Factor 1 is on the x-axis and factor 2 is on the y-axis. In each panel the Faraday population samples are circled.

Table S1. Minor allele frequency (MAF) and *z* score for loci with *z* score < -5 across the whole dataset of 4,179 SNPs genotyped at 365 samples of orange roughy from the Atlantic Ocean

MAF	z.HWE
0.02	-10.00
0.02	-6.76
0.01	-6.26
0.01	-6.26
0.01	-5.33
0.01	-5.30

Table S2. Minor allele frequency (MAF) and *z* score loci with *z* score < -5 identified across 4,179 SNPs genotyped at 365 samples of orange roughy from the Atlantic Ocean sampled from eight separate locations.

Population	MAF	z.HWE
Hebrides	0.02	-6.93
North Rockall	0.02	-6.86
North Rockall	0.02	-6.86
Porcupine Bank	0.03	-5.92
Porcupine Bank	0.13	-5.16
Bay of Biscay	0.02	-6.56
Bay of Biscay	0.02	-6.56
Bay of Biscay	0.02	-6.56
Sedlo Bank	0.08	-5.15
Namibia	0.02	-7.62
Namibia	0.04	-6.02
Namibia	0.12	-5.14
Namibia	0.03	-5.01
Namibia	0.03	-5.01
Namibia	0.03	-5.01
Namibia	0.03	-5.01
Namibia	0.03	-5.01
South Africa	0.01	-8.25
South Africa	0.02	-5.44
South Africa	0.02	-5.39